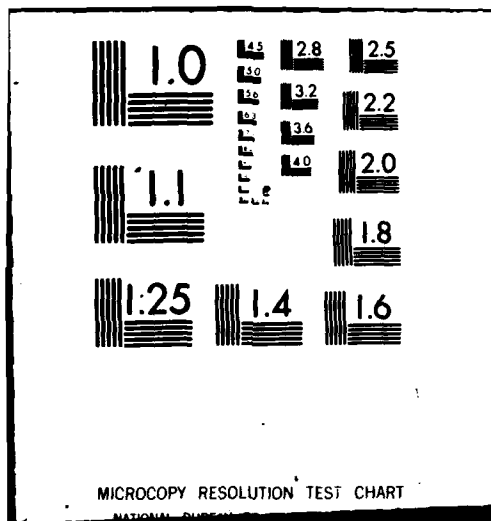


AD-A113 016    NAPLES UNIV (ITALY) DEPT OF CHEMICAL ENGINEERING    F/G 11/9  
EFFECT OF APPLIED STRESS, THERMAL ENVIRONMENT AND WATER IN EPOX--ETC(U)  
DEC 80 L NICOLAIS, A APICELLA, E DRIOLI    AFOSR-77-3369  
UNCLASSIFIED    AFOSR-TR-82-0215    NL

END  
DATE  
ENTERED  
4-82  
DTIC





Report Number

AFOSR-77-3369

EFFECT OF APPLIED STRESS, THERMAL  
ENVIRONMENT AND WATER IN EPOXY RESINS.

L. NICOLAIS  
A. APICELLA  
E. DRIOLI

December 1980  
Final Scientific Report  
01 June 77 - 30 Nov. 1980

Department of Chemical Engineering,  
University of Naples, 80125 Naples  
Italy

Approved for public release.

Prepared for :

UNITED STATES AIR FORCE, AIR FORCE OFFICE  
OF SCIENTIFIC RESEARCH

and

EUROPEAN OFFICE OF AEROSPACE RESEARCH AND  
DEVELOPMENT, LONDON, ENGLAND

MR. FILE COPY

DTIC  
ELECTE  
S APR 6 1982 D  
D

Approved for public release;  
distribution unlimited.

UNCLASSIFIED

**SECURITY CLASSIFICATION OF THIS PAGE (When Data Entered)**

REPORT DOCUMENTATION PAGE		READ INSTRUCTIONS BEFORE COMPLETING FORM
1. REPORT NUMBER <b>AFOSR-TR- 32 -0215</b>		2. GOVT ACCESSION NO. <b>AD-A113 016</b>
3. TITLE (and Subtitle) <b>EFFECT OF APPLIED STRESS, THERMAL ENVIRONMENT AND WATER IN EPOXY RESINS.</b>		4. TYPE OF REPORT & PERIOD COVERED FINAL 01 JUL 77 - 30 NOV 80
5. AUTHOR(s) <b>NICOLAIS APICELLA DRIOLI</b>		6. PERFORMING ORG. REPORT NUMBER <b>AFOSR-77-3369</b>
7. PERFORMING ORGANIZATION NAME AND ADDRESS <b>DEPARTMENT OF CHEMICAL ENGINEERING UNIVERSITY OF NAPLES, 80125 NAPLES ITALY</b>		8. CONTRACT OR GRANT NUMBER(s) <b>2307/B2 61102F</b>
9. CONTROLLING OFFICE NAME AND ADDRESS <b>AIR FORCE OFFICE OF SCIENTIFIC RESEARCH/NA BOLLING AIR FORCE BASE, DC 20332</b>		10. PROGRAM ELEMENT, PROJECT, TASK AREA & WORK UNIT NUMBERS <b>Controlling Office)</b> <b>DEC 1980</b>
		11. REPORT DATE <b>12. NUMBER OF PAGES 49</b>
		13. SECURITY CLASS. (of this report) <b>UNCLASSIFIED</b>
		14. DECLASSIFICATION/DOWNGRADING SCHEDULE
15. DISTRIBUTION STATEMENT (of this Report)  <b>Approved for public release; distribution unlimited.</b>		
16. DISTRIBUTION STATEMENT (of the abstract entered in Block 20, if different from Report)		
17. SUPPLEMENTARY NOTES		
18. KEY WORDS (Continue on reverse side if necessary and identify by block number)  <b>ABSORPTION HYGROTHERMAL MICRODAMAGE SOLUBILITY</b>		
19. ABSTRACT (Continue on reverse side if necessary and identify by block number)  <b>A series of absorption experiments on Epikote 828 resin have been conducted to provide a qualitative understanding of the mechanisms associated with moisture uptake by composite matrix materials, and to assess the effects of the hygrothermal and stress environments. Absorption kinetics and apparent equilibrium moisture concentrations have been determined by immersing samples in constant temperature baths, and periodically removing them for weighing on a quartz helical spring microbalance, until no change in weight could be</b>		

UNCLASSIFIED

SECURITY CLASSIFICATION OF THIS PAGE (When Data Entered)

detected. Two sample types differing in the length of postcuring (3 and 6 days respectively) have been tested to determine the effect of curing on moisture absorption. Both samples behave identically during initial absorption tests. On subsequent drying under vacuum at temperatures above the glass transition temperature, the 3-day cured specimens exhibit dry weights consistently below the original weights (prior to absorption) by amounts of about 0.5%. This is interpreted as indicative of a desorption of low molecular weight components (from either cross linking agent or the monomer) taking place during the swollen state. The six-day cured specimens exhibit no such phenomenon, and have thus been adopted as the standard specimen for all other tests. Absorption tests following prior hygrothermal conditioning have produced interesting results which give credence to the theory of moisture induced micromechanical damage in polymeric resins. Constant temperature absorptions and desorptions have been carried out on the same sample at progressively higher humidity levels. Plots of equilibrium solubilities versus humidity levels have been generated for ambient temperatures ranging from 20°C to 75°C. The curve for a virgin material is non-linear with increasing upward deviation (from an initial tangent line) at humidities above 60%. Subsequent desorption and reabsorption for the same specimen has yielded solubilities which are linear with activity level (relative humidity) at higher levels than in the virgin state for all activity levels less than the maximum attained in the initial exposure. The initial nonlinearity is attributed to micro-damage processes leading to an increase in microvoids and hence higher solubility on subsequent exposures. Microdamage is retarded on subsequent reabsorption following desorption until the highest activity level of pre-exposures has been reached. The microdamage process is also dependent on the ambient temperature. At low temperatures (below 20°C), no microdamage effect has been observed at any activity level. At higher temperatures damage observations have been associated with 50% or higher activity levels.

Accession For	
NTIS GRA&I <input checked="" type="checkbox"/>	
DTIC TAB <input type="checkbox"/>	
Unannounced <input type="checkbox"/>	
Justification	
By _____	
Distribution/	
Availability Codes	
Dist	Avail and/or Special
F	



UNCLASSIFIED

SECURITY CLASSIFICATION OF THIS PAGE (When Data Entered)

## INTRODUCTION

Fiber reinforced plastics are being increasingly utilized for structural applications where their long-term properties are of primary importance. As a result, the problem of the environmental aging on the mechanical performance is attracting a great deal of attention.

In the case of epoxy composites it has been shown that their elevated mechanical properties are strongly affected by moisture absorption from high humidity environments (1-9). This effect, especially at higher temperatures, has been associated with moisture induced plasticization and/or micromechanical damaging (6,7). Sorbed moisture, in fact, acts both as a plasticizer and a crazing agent for the epoxies.

The physical and mechanical integrity of the epoxies is therefore deteriorated by certain thermal-moisture exposure but, while the plasticization is a reversible phenomenon, the microcavitation is not recoverable.

The damaging process, governed by the synergistic action of sorbed moisture and temperature, is particularly evident on water uptakes for which additional weight gains are observed (1,3,6) if samples are exposed to cycling conditions of environment and temperature (thermal spikes).

This additional weight gain has been attributed to moisture entrapment during microcracking of the resin, since glass transition temperature changes were not observed (6). Often, when the diffusing molecules present high affinity for the polymer, the sorption is coupled with molecular relaxation and crazing (10-16) wherein morphological modification of the polymer is involved.

Anomalous sorption behavior has been reported for numerous polymer-diluent systems (13,17,19,22), in particular for thermoplastic polymers, a sharp advancing front has been observed and both the propagation kinetics and morphological modifications due to the solvent have been extensively studied (18,20,22).

AIR FORCE OFFICE OF SCIENTIFIC RESEARCH (AFSC)  
NOTICE OF TRANSMITTAL TO DTIC

This technical report has been reviewed and is  
approved for public release IAW AFR 190-12.  
Distribution is unlimited.

MATTHEW J. KERPER

Chief, Technical Information Division

Low crosslinked polymers have shown almost similar behavior (15). However, the crosslinked structure of these resins reduces the amount of relaxation due to the solvent sorption, which namely may take place in regions with a lower crosslinking density (4,23,25).

Moreover, for sorption of moisture and water, localized cavitation has been primarily focused on the effects of moisture sorption on the properties of thermosetting resins during "thermal spikes" in real-life simulation tests (1,2,5,6,26,27).

The consequent reduction of the ultimate properties has been attributed both to irreversible damage (microcrack formation) and to reversible damage (water plasticization) (6). The formed microcavities may trap additional water without modifying the total amount actually dissolved in the bulk polymer. Equilibrium weight gains have been, indeed, observed (10) to be progressively affected by microcavity formation as the temperature of the water sorption test was increased.

A history dependent solubility model has been previously presented in a form generalized in accordance with the Dual Mode Sorption Theory (24) to take into account the hygrothermal history dependence of the effective diffusion coefficients. Furthermore, the hypothesized morphological changes in the form of microcavities have been correlated to the diffusion parameters. Sorption kinetics of water and moisture in epoxy resins were, in fact, analyzed (30) in the light of a complete immobilization model for the trapped species.

Equilibrium moisture sorptions, usually reported to be represented by phenomenological power law functions of the Relative Humidity with exponents ranging from 1 to 2 or higher values (1,27,31,32), were also interpreted in the light of the proposed model.

On the other hand, since crazing has been associated in glassy polymers with the initiation of brittle fracture, the knowledge of the nature of the

morphological changes occurring in "real life" test conditions is of great interest in the life assessment of composites using epoxies as matrices. The role of sorbed organic solvents in craze and crack initiation has been pointed out by several Authors (33,34). Surface energy reduction and plasticization are mainly involved in void nucleation and growth under the action of a tensile stress.

The influence of an applied stress has been previously studied (35,36) when coupled with the exposure to a humid environment in severe conditions of temperature. A general crazing criterion was used to discuss the nature of the damage induced in the resin when exposed in humid environments under different conditions of temperature and applied stresses.

Moreover, the presence of rigid fillers in a polymeric composite may enhance microvoid formation in regions where stresses are concentrated.

In fact, an applied tensile stress has been found to increase the tendency of the material to nucleate crazes.

## EXPERIMENTAL SECTION

### Materials

Specimens were prepared from Epikote 828 (Shell Co.), using commercial triethylene-tetramine (TETA), (Montedison S.p.A.) as curing agent. Distilled water was used in sorption experiments.

Dissolved gases were removed by repeated freeze-thaw cycles, under vacuum, using liquid nitrogen as refrigerant.

### Preparation of Samples

The resin and crosslinking agent were hand-mixed at room temperature in a 100 to 14 ratio without further purification, and then vigorously mixed under vacuum for 15 min., without any appreciable loss of TETA. The mixture was then poured into PMMA moulds of 0.60 to 3.00 mm thickness, kept under vacuum for 1h to degas the system completely and then kept in a dry atmosphere at 23°C for 24h.

Curing was initiated at 80°C under vacuum for 24h and finally the temperature was brought to 100°C for a curing stage of 3 days. A second batch of samples was prepared in an identical manner; however, the final curing period was increased to 6 days.

Samples were subsequently stored in a dessicator containing anhydrous  $\text{CaCl}_2$  before determining the effects of hygrothermal history on the resin properties.

Glass bead composites were prepared using Vacu-Blast glass microspheres with particle sizes in the range of 32 to 40 microns. The glass microspheres were first cleaned in solvents to eliminate dirt and other unwanted organics on the surfaces. A 7.5% by volume composite was studied.

### Sorption Kinetics Experiments

Moisture sorption kinetics and apparent equilibria were determined by means of a Mc Bain (37) quartz, helical spring microbalance served by a standard vacuum system. The quartz springs with a 0.50 mg/mm sensitivity were obtained from the Ruska Corporation, Worden Quartz Products Division, Houston, Texas. The sample temperature was maintained constant by circulating thermostated water through a water jacket surrounding the sorption cell. Different activities have been maintained in the system by imposing and controlling, by means of a mercury differential manometer, different pressures of water vapors.

Gravimetric liquid sorption measurements were performed by weighing  $3.0 \times 3.0 \times 0.05 \text{ cm}^3$  samples repeatedly on a Galileo analytical balance following immersion in water maintained at constant temperature. The samples were removed from the water, blotted, placed in a weighting bottle, weighed and finally replaced in the constant temperature water bath.

Sorption data are indicated as C (percentage of weight gain referred to the dry weight) and plotted as a function of  $t^{1/2}/l$ , where l is the thickness of the samples ranging from 0.2 to 0.4 mm for vapor sorption and from 0.4 to 0.6 mm for liquid sorptions.

Liquid sorptions on specimens subjected to a different "stress history" have been performed by suspending in thermostated water dumbbell-shaped samples which were kept in tension by using a dead load. Unloaded reference samples were also equilibrated in the same pool. When the reference samples had reached water saturation, the central portion of the loaded dumbbell was cut, weighed in the wet state, and dried under vacuum at the same temperature of the sorption test. Liquid water resorptions were then followed by gravimetric measurements on the previously loaded and unloaded samples.

### Mechanical procedures

Clash-Berg experiments; mechanical tests were performed by using a

Clash-Berg torsional stiffness apparatus.

Untreated specimens, 60x10x3.0 mm<sup>3</sup> and otherwise identical samples, previously immersed and saturated in water at two temperatures (75° and 45°C), were subsequently tested over a broad range of temperatures while the specimen was completely submerged in paraffin oil. The angular deflection  $\alpha$ , was measured after application of a torque,  $M_t$  for 10 seconds.

The values of the shear moduli were calculated according to the following equation:

$$G(10) = 917 \frac{M_t l}{u a b}$$

where a,b and l are, respectively, the width, thickness and length of the specimen and u is a tabulated parameter which depends upon the ratio a/b (10).

Stress-strain experiments; specimens, in dumbbell shape, with thickness of 0.6 mm, a minimum width of 5 mm and a distance between the grips of 5 cm, were loaded in tension by the Instron tester equipped with a temperature controlled chamber for dry tests and with a thermostatically controlled water bath for tests on saturated samples. Constant strain rate of about 0.1 min.<sup>-1</sup> was used..

ENVIRONMENTAL AGING OF EPOXY RESINS: INVESTIGATION ON SOME MICROSTRUCTURAL FEATURES LEADING TO CHANGES OF THE BULK PROPERTIES.

Development of a diffusion technique to investigate bulk morphological modifications.

Diffusion of small molecules in glassy polymers is often associated to morphological modifications of the bulk material. This fact involves sorption kinetics which are reported as "anomalous". Since extensive studies have been carried out on the characterization of the physical events occurring during sorption (10,16,33), it has been possible to relate its particular behavior to structure modifications.

The presence of microcavities in damaged epoxy resins has been related to the effective diffusion coefficients by using for the Languimirian population history dependent hole saturation constants (29).

The Dual Mode Sorption Theory has been successfully developed to correlate the presence of hypothesized "pre-existing holes" or "free volume elements" frozen in the glassy state to characteristic anomalous sorption behaviors of gasses and vapours in glassy polymers. If changes of the apparent water solubilities after aging are attributed to a microcavita-tional damage of the size of the nucleating crazes (33), the increase of the number of high energy sorbing sites in which the diffusing molecules may be trapped and immobilized, should be then evident in a reduction of the effective diffusion coefficient following the increase of the Langui-mirian capacity (28).

Sorption Kinetics Model

Assuming that the equilibrium concentration of the penetrating spe-cies in the glassy polymer may be separated in two terms, one history independent and the other history dependent, one may write:

$$C_r(T, \tau, a, \alpha) = C_1(T, a) + C_2(T, \tau, a, \alpha) \quad (1)$$

where  $T$  and  $a$  are the actual temperature and external activity, and  $\alpha$  and  $\tau$  are the previous thermal and activity history. In addition, considering that  $C_1$  may be described by the combination of a Henry's law dissolved term and a Langmuir "preexisting hole filling" term in accordance with the Dual Mode Sorption Theory (28,29)

$$C_1 = k_d(T)a + \frac{C'_{ho}b(T)a}{1 + b(T)a} \quad (2)$$

where  $k_d$  is the Henry's law constant for dissolved species,  $a$  is the external activity and  $C'_{ho}$  and  $b$  the Langmuir capacity constant for preexisting holes and the affinity constant, respectively.

Due to the microcavitations nature of the hypothesized damage, the history dependent solubility term is assumed to be of Langmuir type only:

$$C_2(T, \tau, a, \alpha) = \frac{C'_h(\tau, \alpha)b(T)a}{1 + b(T)a} \quad (3)$$

where  $C'_h$  is the hole saturation constant which is associated with the induced cavities in the polymer and  $b(T)$  the polymer-diluent affinity constant, which is the same as the one reported in Eq. 2. Substituting Eqs. 2 and 3 in 1, one obtains:

$$C_1(T, \tau, a, \alpha) = k_d(T)a + \frac{[C'_{ho} + C'_h(\tau, \alpha)]b(T)a}{1 + b(T)a} \quad (4)$$

In the case of linear isotherm, where  $ab \ll 1$ , Eq. 4 becomes:

$$C_1 = [K(T) + K'(\tau, \alpha)]a \quad (5)$$

where

$$K(T) = k_d(T) + C'_{ho}b(T) \quad (5')$$

and

$$K'(\tau, \alpha) = C'_h(\tau, \alpha)b(T) \quad (5'')$$

For experiments performed at constant temperature and fixed external activity  $C_T$  will be only a function of the previous hygrothermal history.

The transport model for systems in which sorbed molecules can be divided into two populations, one formed by completely immobilized molecules and the other by molecules free to diffuse, has been developed by Vieth and Sladek (38) in a modified form of Fick's second law. Subsequently a partial immobilization model has been successfully developed by Paul and Koros (31) from the relaxation of the postulate of complete immobilization also suggested by Petropoulos (40).

Due to the strong interactions between the penetrant and the polymer and the high cohesive energy of water, large differences in relative mobilities are expected and the total immobilization model has then been used. In such a case, in fact, when linear sorption isotherms are experimentally found, diffusion of a penetrant may be described by the classic diffusion law with constant value of the effective diffusion coefficient (41):

$$D_{eff} = \frac{k_d}{K_T} D \quad (6)$$

where  $k_d$  and  $K_T$  are respectively the true and the overall apparent Henry's law constant and  $D$  the actual diffusion coefficient of the dissolved species.

Equation 6 states that when part of the diffusing molecules are immobilized, the effective diffusion coefficient is lower than the actual. Once the isotherm 5 is irreversibly fixed by the previous history ( $K' =$  constant), it is linear and  $K_T$  becomes:

$$K_T = K + K' \quad (7)$$

where  $K$  and  $K'$  are defined in Eq. 5' and 5".

Since  $k_d$  cannot be directly calculated, Eq. 6 has been primarily used to investigate the nature of the morphological changes associated with water sorption. In fact, in the case of microcavitations damage, samples damaged

by different amounts will show different effective diffusion coefficients and solubilities, also if tested in the same experimental conditions. By indicating with the superscript prime and double prime the higher and the lower degree of damage respectively, one can write (from Eq. 6) :

$$\frac{D'}{D''} = \frac{K_r''}{K_r'} \quad (8)$$

In the case of irreversible microcavitation nature of the damage Eq. 8 is verified when for high apparent solubilities, lower effective diffusion coefficients are experimentally found.

Moreover, classic Fickian diffusion laws for constant diffusion coefficients are not expected to adequately describe water sorption in epoxy resins during the damaging process.

This is, in fact, mathematically equivalent to the case of concentration dependent diffusion coefficients, due to the history dependence of  $K'$  in Eq. 6.

Such technique has been tested on samples with different aging histories (30) giving good supports to the hypothesis of the nature of the damaging process.

Some aspects on the possible levels of damage induced by hygrothermal conditioning are summarized in the following.

#### Effects of Postcuring

Mechanical results in torsion experiments for the two batches of samples are reported in Figure 1. Mechanical tests do not reveal any significant difference between the samples postcured for 3 and 6 days. Water sorption data for samples postcured for 3 days are reported in Figure 2. The four curves refer to sorption into samples immersed in liquid water at four temperatures: 23°, 45°, 75° and 90°C.

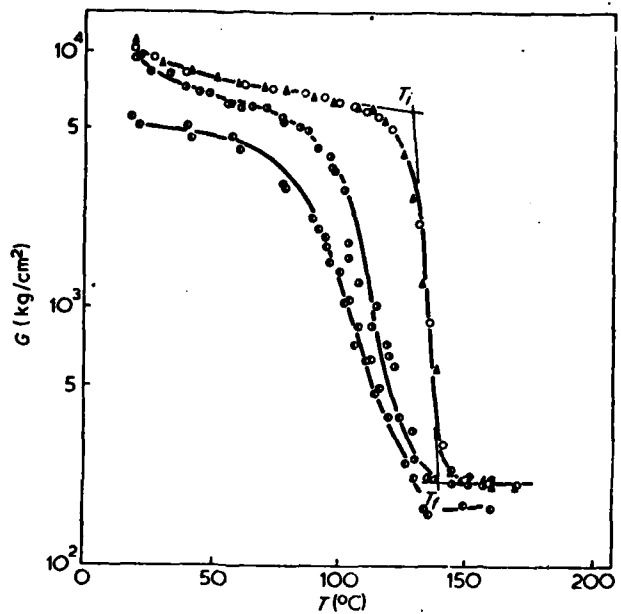


Figure 1 Torsional test results for dry samples: ▲, 6 days cured samples; ○, 3 days cured samples; ●, saturated 75°C; ◉, saturated 45°C.  $T_g = (T_i + T_f)/2$

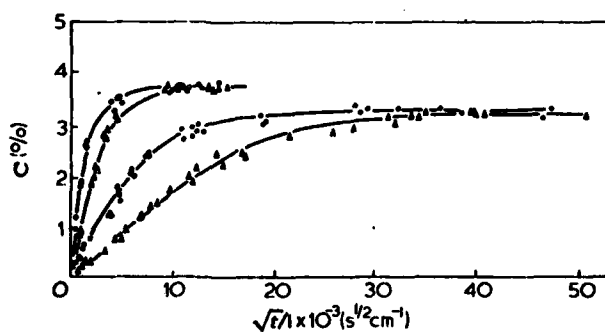


Figure 2 Sorption behaviour of 3 days cured samples as prepared. Solid triangles: 23°C. Solid circles: 45°C. Open triangles: 75°C. Open circles: 90°C

Some of the samples, first preswollen in water at 90°C for two weeks, were dried under vacuum at temperatures above the glass transition for 24h, and then weighed again in the dry state.

The weight after such a treatment was systematically below the original weight, by an amount of between 0.4 and 0.5%. This suggests that desorption of some low molecular weight component (which may be either the crosslinking agent or the monomer or both) may take place in the swollen state during the sorption test.

If indeed that is so, the weight increase observed during sorption may be the difference between the water sorbed and the low molecular weight component desorbed so that the data in Figure 2 may, in fact, be misleading.

Figures 3 and 4 report sorption data at 23° and 45°C respectively, for samples postcured for 3 days.

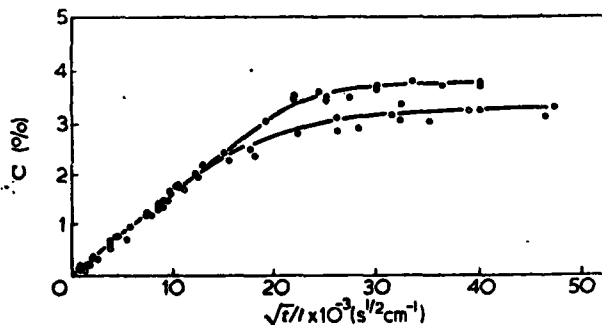


Figure 3 Sorption behaviour at 23°C for 3 days cured samples. Open circles, samples as prepared. Solid circles, samples previously swollen and dried

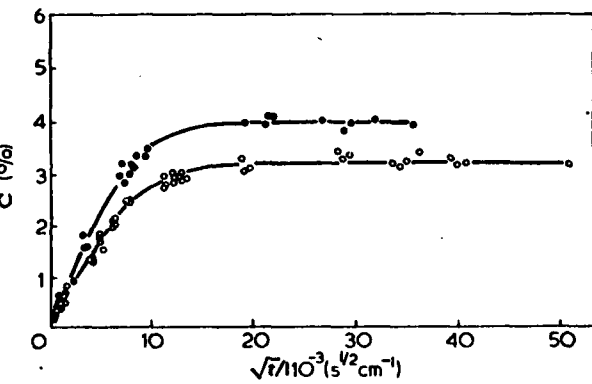


Figure 4 Sorption behaviour for 3 days samples at 45°C. Open circles as prepared. Solid circles, samples previously swollen and dried

The two curves in each Figure refer to the sample "as-prepared" (lower curve), and to the sample after the preswelling-drying procedure. The difference between the final asymptotic values is indeed of the order of 0.5%, which supports the idea that desorption of the low molecular weight component takes place at the same time as water sorption in "as-prepared" samples. At 45°C (Figure 4) the two processes appear to be about equally as fast, since the two curves are separated both in the kinetics and the asymptotic regions; at 23°C (Figure 3) desorption appears to be slower than water sorption.

No such phenomena have been observed with samples postcured for 6 days, which did not exhibit any measurable weight loss when exposed

to the preswelling-drying cycle. The sorption behavior of samples "as-prepared", and of samples which had undergone the preswelling-drying cycle was identical. These results suggest that 6 days of postcure at 100°C are required to completely cure the epoxy. Good reproducibility was obtained for the sorption behavior of such samples in several different tests. All the results discussed in the following refer to 6 days postcured samples.

#### Effects of Hygrothermal History

Water sorption data in 6 day cured samples at 23°, 45° and 75° are reported in Figure 5.

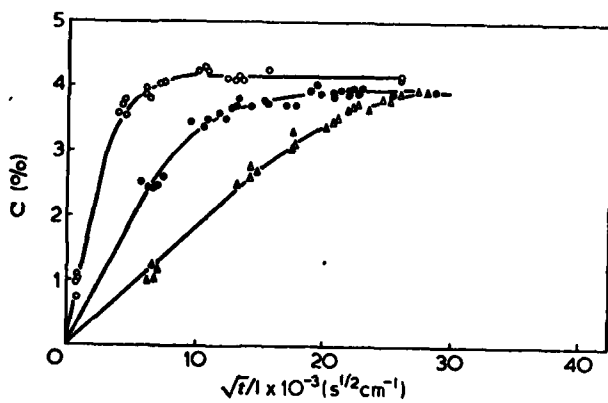


Figure 5 Sorption behaviour for 6 days cured samples. Open triangles, 23°C. Solid circles, 45°C. Open circles, 75°C

The final asymptotic value of the apparent solubility, C is a weakly increasing function of temperature. The kinetic behavior appears to be described adequately by ordinary diffusion, since a finite initial slope is exhibited by the sorption curves in the C vs  $t^{1/2}/l$  diagrams. Moreover, data obtained on films with varying thickness superimpose on a C vs  $t^{1/2}/l$  diagram (though the range of thickness investigated is not very wide, 0.4mm < l < 0.7mm) can extract an apparent diffusion coefficient from the initial slope by making use of the classical early time approximation:

$$\frac{C_t}{C_\infty} = \frac{4}{\pi^{1/2}} \left( \frac{Dt}{l^2} \right)^{1/2} \quad (9)$$

where  $C_\infty$  is the asymptotic value of C and D is the apparent diffusion coefficient.

An Arrhenius plot of diffusion coefficients obtained from the initial slopes of the curves in Figure 5 gave a straight line drawn through the three data points; the corresponding activation energy is 13.3 Kcal/mol.

While the solubility values at  $23^\circ\text{C}$  and  $45^\circ\text{C}$  are not significantly different, the value at  $75^\circ\text{C}$  is certainly higher than the other two. We would therefore expect that a sample brought to equilibrium at  $75^\circ\text{C}$  would exhibit water desorption if brought to  $23^\circ\text{C}$  at a later stage.

When this experiment was performed, however, the opposite behavior was observed, as shown in Figure 6.

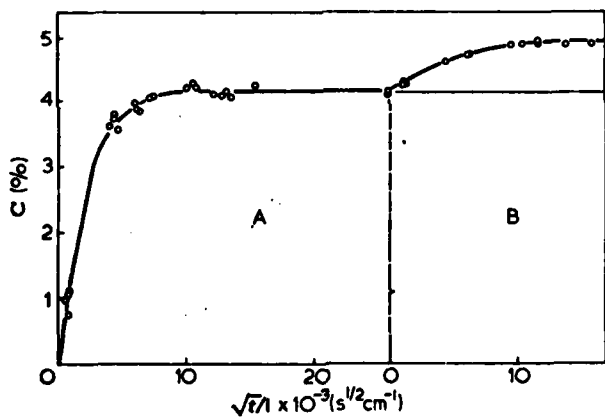


Figure 6 Sorption behaviour at  $23^\circ\text{C}$  (B) of a sample previously equilibrated at  $75^\circ\text{C}$  (A)

The sample had apparently reached equilibrium at  $75^\circ\text{C}$ ; when brought down to  $23^\circ\text{C}$  significant additional sorption of water occurred. The new value of the apparent solubility at  $23^\circ\text{C}$  is 4.86% as compared to 3.92% observed in the virgin sample.

Figure 7 shows, on an expanded scale, the additional sorption at  $23^\circ\text{C}$  of a sample previously equilibrated at  $75^\circ\text{C}$  (open circles).

When the same sample is brought back to  $75^\circ\text{C}$ , water desorption takes place and the final apparent solubility is the same of a virgin sample,

i.e. 4.12%. If a sample is first equilibrated at 23°C, then at 75°C, and then again at 23°C, its behavior (full circles) is the same as that of a sample just equilibrated once at 75°C. It appears that the only relevant parameter of the hydrothermal history of the sample is the highest temperature at which it has been equilibrated with water. A similar analysis has been made for 75°-45°-75°C and 45°-23°-45°C cycles.

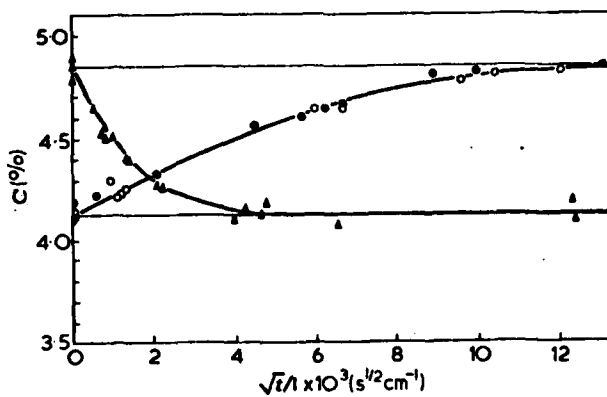


Figure 7 Sorption behaviour at 23°C of a sample previously equilibrated at 75°C (open circles). Desorption behaviour when same sample is brought back to 75°C (triangles). Sorption at 23°C with different temperature history, see text (solid circles)

FIRST TENTATIVE INTERPRETATION OF THE RESULTS

The experimental results discussed so far clearly indicate the influence of a hygrothermal history on the apparent sorption equilibria. Such history-dependent apparent equilibria have been discussed in the literature, and it has been suggested, also in more general terms, that history-dependent thermodynamics may be approached from the viewpoint of internal or hidden, state variables. Such an approach has been explicitly considered for the modelling of diffusion behavior in polymeric solids. Specifically, we may assume that the state of the sample may be identified (in addition to the usual state variables such as temperature and pressure) by at least one additional state variable .

For the phenomena considered here, a concrete physical interpretation for the internal state variable  $\chi$  may be suggested:  $\chi$  may be regarded as the volume percent of microcavities which may form in the sample under combined action of temperature and humidity.

This specific physical identification of  $\chi$  , however, is not crucial to the subsequent analysis, and although we will refer to volume percent microcavities in the following, we do not claim to have definite experimental proof that such microcavities do form, though physical support for this kind of interpretation of  $\chi$  is discussed below.

This apparent solubility in any given sample,  $C_{\infty}$  , may be regarded as the sum of two terms, the first one,  $C_p$  , representing the equilibrium content of water in the compact resin, and the second,  $C_2$  , representing the amount of water which may be present in the microcavities:

$$C_{\infty} = C_p + C_2$$

$C_2$  is equal to  $\rho \chi$  , where  $\rho$  is the density of the water at that temperature and  $\chi$  the volume fraction of microcavities.

Assuming a standard state at  $23^{\circ}\text{C}$  in which  $C_2 = 0$  and also that the rate of formation of microcavities at  $75^{\circ}\text{C}$  is sufficiently fast, so that while sorption proceeds to apparent equilibrium the value of  $C_2$  also reaches some equilibrium value  $C_2^{75}$ .

A sample previously equilibrated at  $75^{\circ}\text{C}$  is characterized by a value  $C_2 = C_2^{75}$ , while a virgin sample is characterized by  $C_2 = 0$ .  $C_2^{75}$  can be then calculated as  $C_{\infty} (23) = 4.86\% = C_p (23) + C_2^{75}$ , but  $C_p (23)$  is obtained from  $C_{\infty}^{23} (23) = C_p (23) = 3.92\%$ , being  $C_2^{23} = 0$  by definition then:  $C_2^{75} = 4.86\% - 3.92\% = 0.94\%$ . The temperature of measurement is given in brackets and the equilibrating temperature is given by a superscript.

A similar analysis on  $C$  at  $23^{\circ}$  for virgin and first equilibrated at  $45^{\circ}\text{C}$  samples yields for  $C_2^{45}$ , the equilibrium microcavities vol.% at  $45^{\circ}\text{C}$ , the value 0.23%. It may be observed that a definite decreasing trend is observed with increasing temperature for the calculated values of  $C_p$  reported in the sixth column of Table I, while no such regular trend is observed for the entries in the second column.

Assuming that the density of water is constant and unity we will have:  $C_2 = x$ .

Table 1 Effect of temperature and prior history on the apparent sorption equilibria

Temperature ( $^{\circ}\text{C}$ )	$C_{\infty}$ for virgin sample, (%)	$C_{\infty}$ for sample first equilibrated at $75^{\circ}\text{C}$ (%)	$C_{\infty}$ for sample first equilibrated at $45^{\circ}\text{C}$ (%)	Calculated volume void fractions (%)	Calculated $C_p$ (%)
23	3.92	4.86	4.15	0	3.92
45	3.90	4.60	3.90	0.23	3.67
75	4.12	4.12	—	0.94	3.18

An alternative interpretation can be suggested from the previous literature on relaxation phenomena occurring in the swollen state.

Samples allowed to be saturated in water at high temperatures can show a more relaxed glassy state compared with that of samples saturated at low temperatures. In the more relaxed state, water sorption can take place when the water environment is cooled to a lower temperature. The

tentative interpretation based on microvoid formation would need to be subjected to scrutiny. The following points are offered as support:

- 1) The difference between the two values of  $C_2^{75} = 0.94$  and  $C_2^{45} = 0.23$  is 0.71%. This compares very favorably with the different apparent solubilities at 45°C observed in the 45°-75°-45° cycle:  $C_{\infty}^{75} (45) - C_{\infty}^{45} (45) = 4.60\% - 3.90\% = 0.70\%$ .
- 2) Clash-Berg mechanical tests have been performed on samples previously saturated with water, at temperatures of 75° and 45°C. The results are reported in Figure 1. We can notice that shear modulus drop above  $T_i$  (initial glass transition temperature as defined in Figure 1) takes place for dry samples within a small temperature range while the range becomes larger for saturated samples.

This can be interpreted as favoring water desorption from the samples during testing times, at temperatures above the initial glass transition temperature.

Water desorption at temperatures below  $T_i$  can be assumed to be negligible in relation to the still glassy state of the system. This assumption seems to be confirmed by the fact that  $T_i$  for the dry system, as for those saturated at 75° and 45°C, are well separated in the temperature scale while  $T_f$ , the final glass transition temperatures, are quite coincident.

Glass transition temperatures for saturated samples, reported in Table 2, can be calculated as  $T_i + \Delta T/2$ , where  $\Delta T$  is the value ( $T_f - T_i$ ) extracted for dry samples.

Table 2

Samples	$T_g$ (°C)	$C_g$ (%)
Dry	135	0.0
Saturated, 75°C	108	3.18
Saturated, 45°C	88	3.63

It may be observed that the samples saturated at 45°C show lower moduli and glass transition temperatures than those saturated at 75°C, in spite of the more plasticized state that can be expected because the value of  $C_w$  at 45°C (3.90%) is less than the value at 75°C (4.12%). Yet, if microcavities are formed, we would expect that only the water actually dissolved in the compact resin (the value of  $C_p$ ) is responsible for the plasticizing action; and indeed the value of  $C_p$  at 45°C (3.63%) is larger than the value at 75°C (3.18%).

3) The largest value of  $\alpha$  reported in Table I is 0.94%; this value is not expected to change the mechanical properties significantly: the shear modulus would only decrease about 3% (42), well below experimental accuracy.

4) Stress-strain mechanical tests on dry and previously equilibrated 75° and 45°C samples have also been performed. For saturated sample tests have been run in a water environment to avoid moisture desorption. At a temperature of 75°C (Figure 8) a brittle behavior for dry and 75°C saturated samples has been observed, in accordance with the shear moduli and glass transition temperatures calculated from Figure 1.

Water content changes in samples saturated at 45°C and exposed to a water environment at 75°C were calculated to be negligible in the short stress-strain time test.

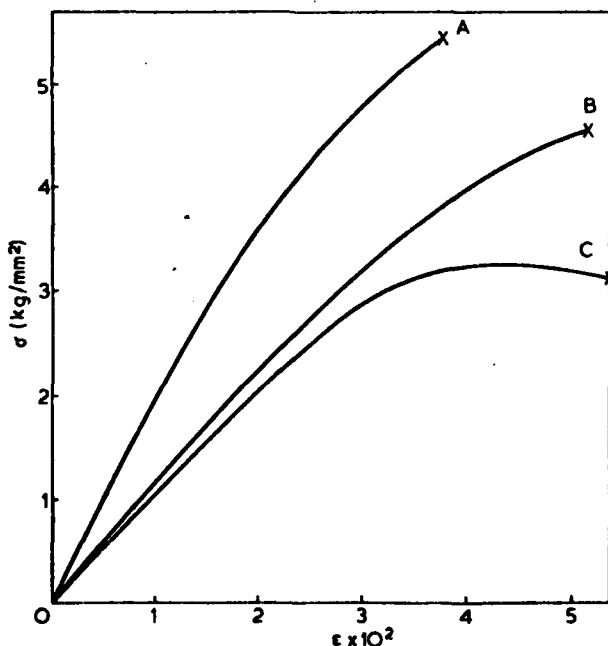


Figure 8. Stress-strain curves at  $T = 75^\circ\text{C}$  for A, dry; saturated at B, 75° and C, 45°C in epoxy resin samples

5) Stress-induced crazing in epoxy resins and in various glassy systems has been reported in the literature (15,33). Furthermore, the energy required for the craze formation is known to decrease with increasing temperature (34).

Therefore, the interpretation based on the formation of microcavities, favored at higher temperatures, is in agreement with the available information.

A sample previously equilibrated at 75°C, dried and brought to temperatures above the glass transition temperature, exhibits the same sorption behavior as virgin samples. It is indeed physically intuitive that any microcavities which may have formed would disappear through the annealing process.

It was observed that water saturation levels in epoxy resins exposed to liquid environments were determined by the highest temperature of the thermal cycles to which samples were subjected in presence of sorbed moisture. The differences in the solubilities of samples with different hydrothermal histories were explained in terms of craze cavities that could be formed by solvent crazing in the plasticized system exposed to high temperatures and which trap additional water (free). As a result, the moisture actually dissolved was found a decreasing function of the temperature also if the water uptakes increased by increasing temperatures.

Nevertheless, higher glass transition temperature depressions were found for samples conditioned in lower temperature environments irrespective of the apparently lower water solubilities. The higher plasticization of the lower temperature conditioned samples was also confirmed by mechanical tests.

DEPENDENCE OF THE SORPTION BEHAVIOR ON THE RELATIVE HUMIDITY HISTORIES

Sorption equilibrium

Constant temperature sorptions and desorptions have been carried out on the same sample at progressively higher humidity levels. Once the sample has been equilibrated at the highest humidity level, a second set of sorptions and desorptions have been followed. The temperatures studied were  $75^{\circ}$ ,  $60^{\circ}$ ,  $45^{\circ}$ ,  $30^{\circ}$ ,  $20^{\circ}$  and  $2^{\circ}$ C (30).

Figure 9 shows polymer weight gains, expressed as grams of water per 100 grams of dry resin, as function of the square root of time normalized to the sample thickness,  $l$ , in experiments performed at  $75^{\circ}$ C. Numbers on the curves refer to the activity at which the specific test has been run. The activity is defined as the ratio between the water vapour pressure in the sorption cell and the saturated water vapour pressure at the temperature of the experiment. For activities higher than 0.60, first sorption experimental points (full circles in Fig. 9a) have been reported since the initial part of the curve does not follow the classical Fickian diffusion predictions (43). Conversely in Figure 9b, sorption and desorption kinetics have been reported for all activities.

In Figure 10, equilibrium solubilities at  $60^{\circ}$ C, obtained from the asymptotic values of the sorption curves both for the first and the second set of sorptions, are reported for different values of the external penetrant activity.

Open circles refer to the progressive moisture weight gains which have been reached in the first set of sorptions. The isotherm is clearly not linear (upward) showing positive deviations from linearity at higher activities. Once the maximum value of external relative humidity has been experienced by the sample, the equilibrium water uptakes were linear with the activities (full circles).

The differences in the sorption behavior, for the same environmental conditions, may be associated to a progressive damage that is produced in

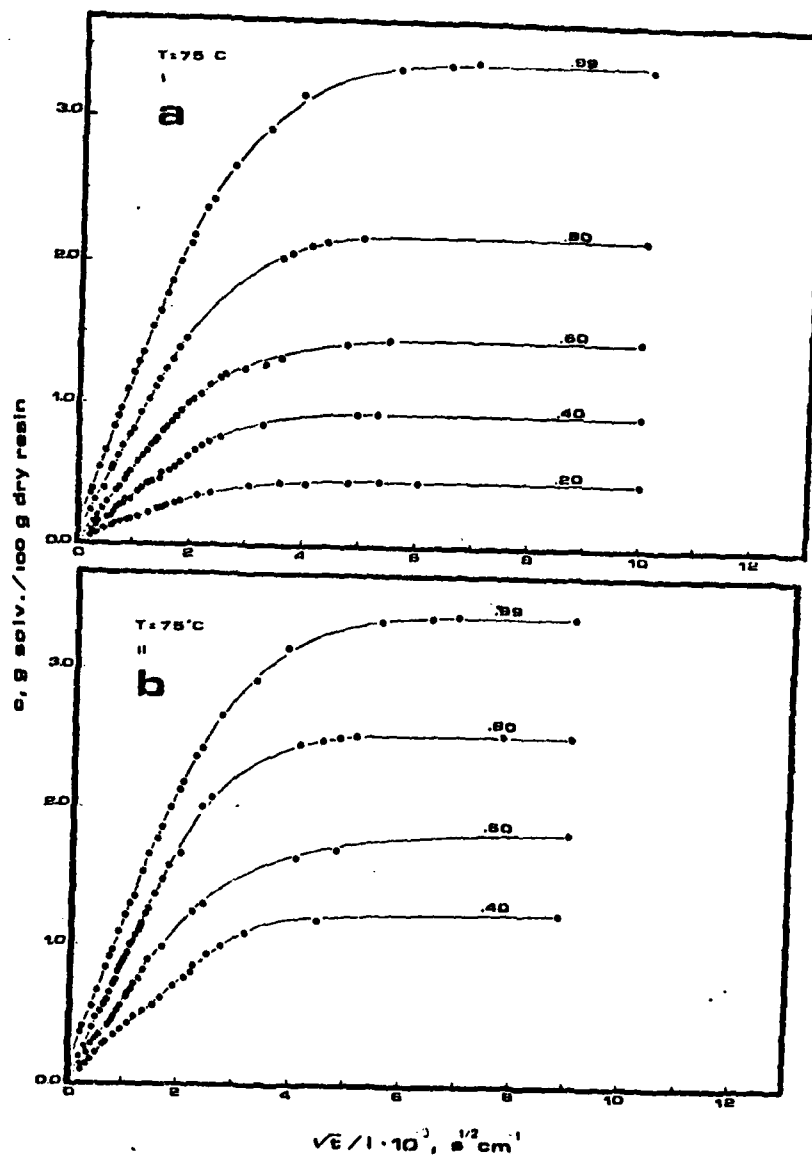


Figure 9: First (a) and second (b) sorption and desorption kinetics from the water vapour phase in epoxy films.

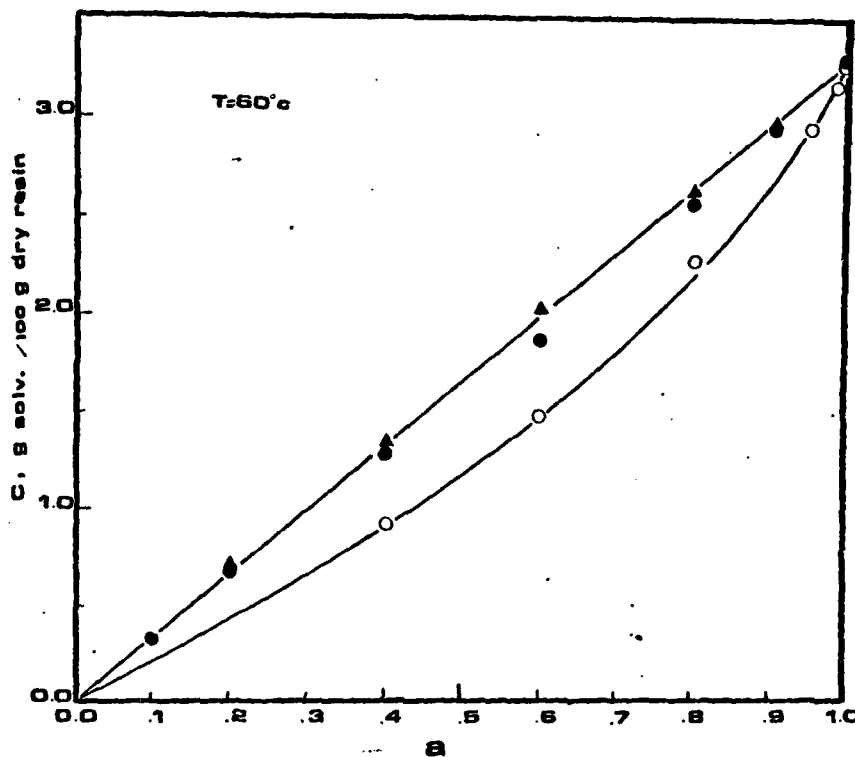


Figure 10: Equilibrium solubility isotherms at 60°C for the first (O), second (●) and third (▲) sorption-desorption cycle sets.

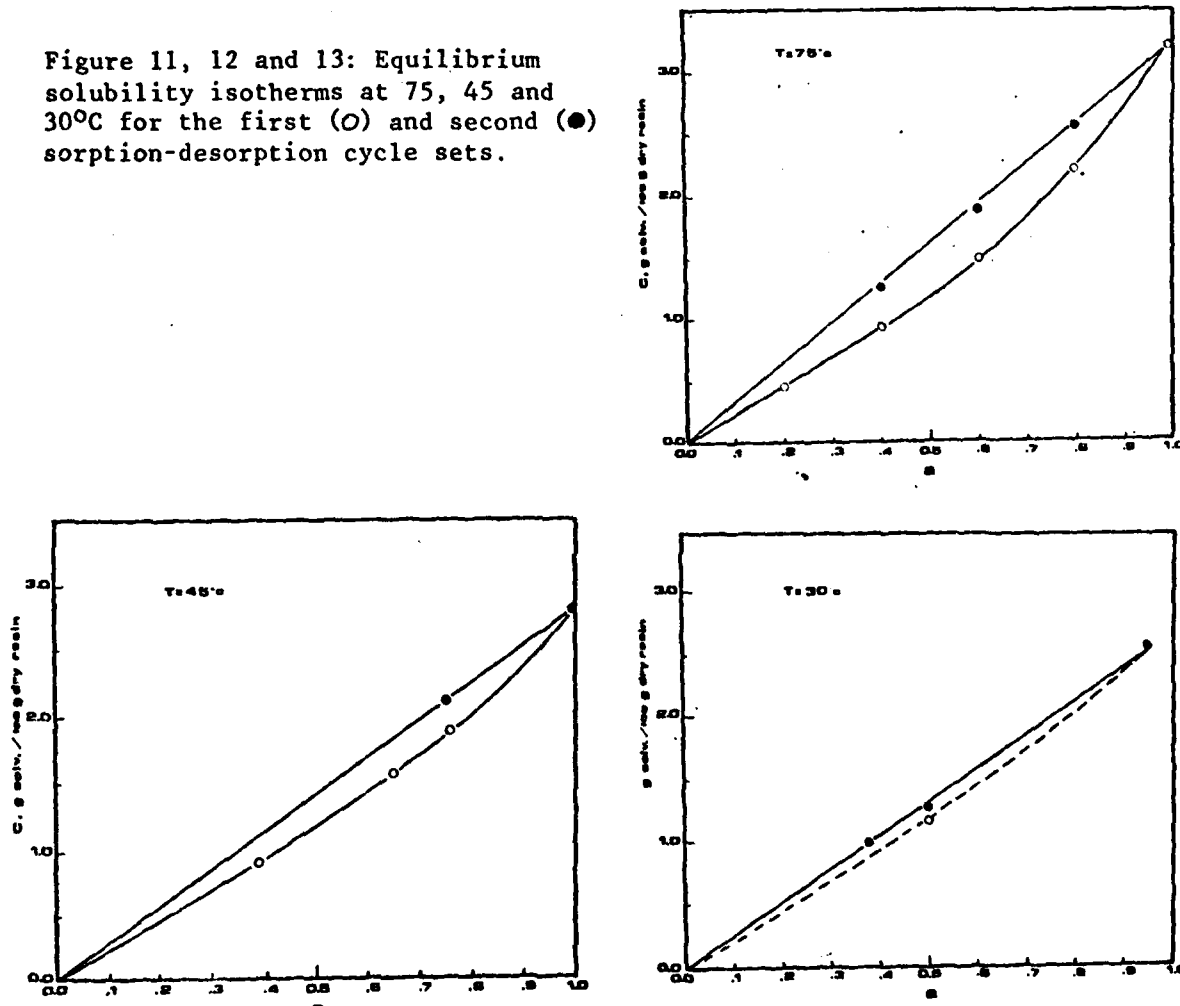
the material equilibrated at increasingly higher moisture contents. Once the maximum equilibrium moisture content has been achieved and the temperature is not increased, no additional damage should be induced in the resin. The polymer-water system then behaves linearly since the internal state of the material does not change during the subsequent experiments. In this case an apparent Henry's law constant might be defined as the slope of the equilibrium linear isotherm. The overall system is then identified by an additional internal state variable which is a function of both the temperature and the moisture content.

Once the system is fixed, the sorption kinetic becomes a reversible phenomenon. In fact, the equilibrium values of the solubility for a

third set of sorption experiments, reported in Figure 10 as full triangles, show a good agreement with the previous data.

The same procedure has been followed for temperatures both higher ( $75^{\circ}\text{C}$ ), Fig. 11, and lower ( $45^{\circ}\text{C}$  and  $30^{\circ}\text{C}$ ), Fig. 12 and 13, than the previous one.

Figure 11, 12 and 13: Equilibrium solubility isotherms at  $75^{\circ}\text{C}$ ,  $45^{\circ}\text{C}$  and  $30^{\circ}\text{C}$  for the first (○) and second (●) sorption-desorption cycle sets.



Upward isotherms relative to the first set of sorption equilibrium solubilities showed at  $75^{\circ}\text{C}$ ,  $45^{\circ}\text{C}$  and  $30^{\circ}\text{C}$  an initial apparently linear part followed by progressive positive deviations for activities higher than 0.60. The possibility of the existence of an apparently initial linear region is in agreement with previous observation (36) indicating that at low moisture contents, irrespectively of the test temperature, the damage induced in the resin is irrelevant.

The Henry's constant obtained on the "as cast" polymer at low activities from the initial slope of the sorption isotherm should be then referred as relative to an undamaged state. Once the samples has been equilibrated at the highest humidity level, the system behaves linearly for all activities and temperature studied with overall higher apparent Henry's law constant than in the undamaged state (initial slope of the upward isotherm).

At lower temperatures, 45° and 30°C, the differences between the linear and the upward isotherms have been described to be less pronounced according to the temperature dependence of the damage in the resin-water system, (Section A). Low temperature environments are, in fact, inducing a lower damage than a higher temperature environment even in the same conditions of moisture content, then the less pronounced humidity history dependence of the apparent solubilities.

Moisture "per se" is not effective in producing any microcavitation in the resin but, as already pointed out in the literature (1,6), the synergistic effect of moisture and temperature is really effective in the damaging process.

For temperatures lower than 30°C (in particular 20°C and 2°C) sorption from liquid phase  $a = 1.00$ , has been followed and the data are reported in Fig. 14.

In Figure 15, water solubilities in resins previously equilibrated at high humidity levels as function of actual vapour pressures (in mm of Hg) and for different temperatures, are shown. For experiments made in the liquid phase, saturated water vapor pressures at the temperature of the tests are used as abscissa, while for tests performed in the vapour phase isotherms break at a pressure equal to the relative saturated water vapor pressures.

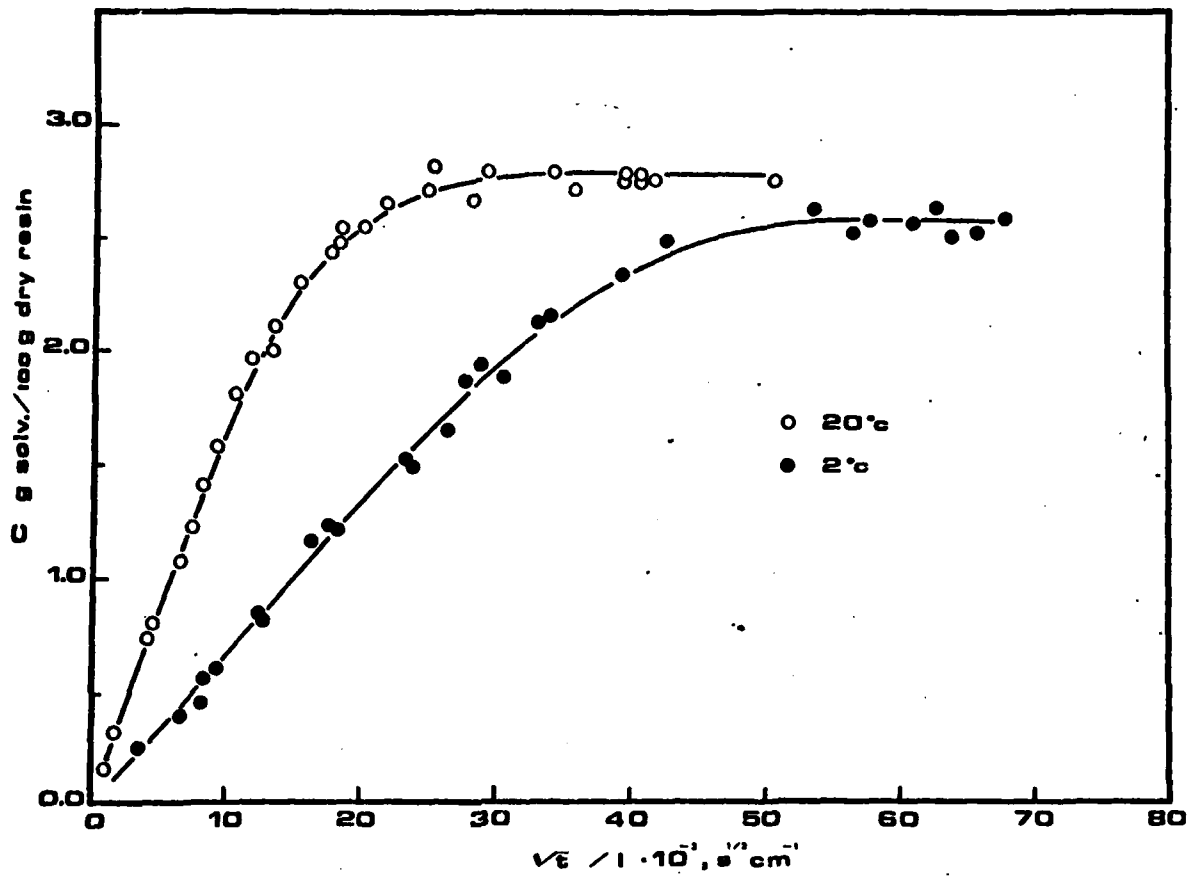


Figure 14: Weight gain as a function of time for water sorption from the liquid phase at 20°C and 2°C.

The overall apparent Henry's law constants  $K$ , calculated from Fig. 15, are plotted in the van't Hoff diagram of Fig. 16 (full circles). On the same Figure apparent Henry's law constants for undamaged resin, which have been obtained from the initial slope of the upward isotherms, are also reported (open circles). Specimens equilibrated at high humidities and at different temperatures are not expected to show apparent Henry's law constant that can be correlated by a straight line in a van't Hoff diagram (full circles) since they possess different degrees of bulk damage.

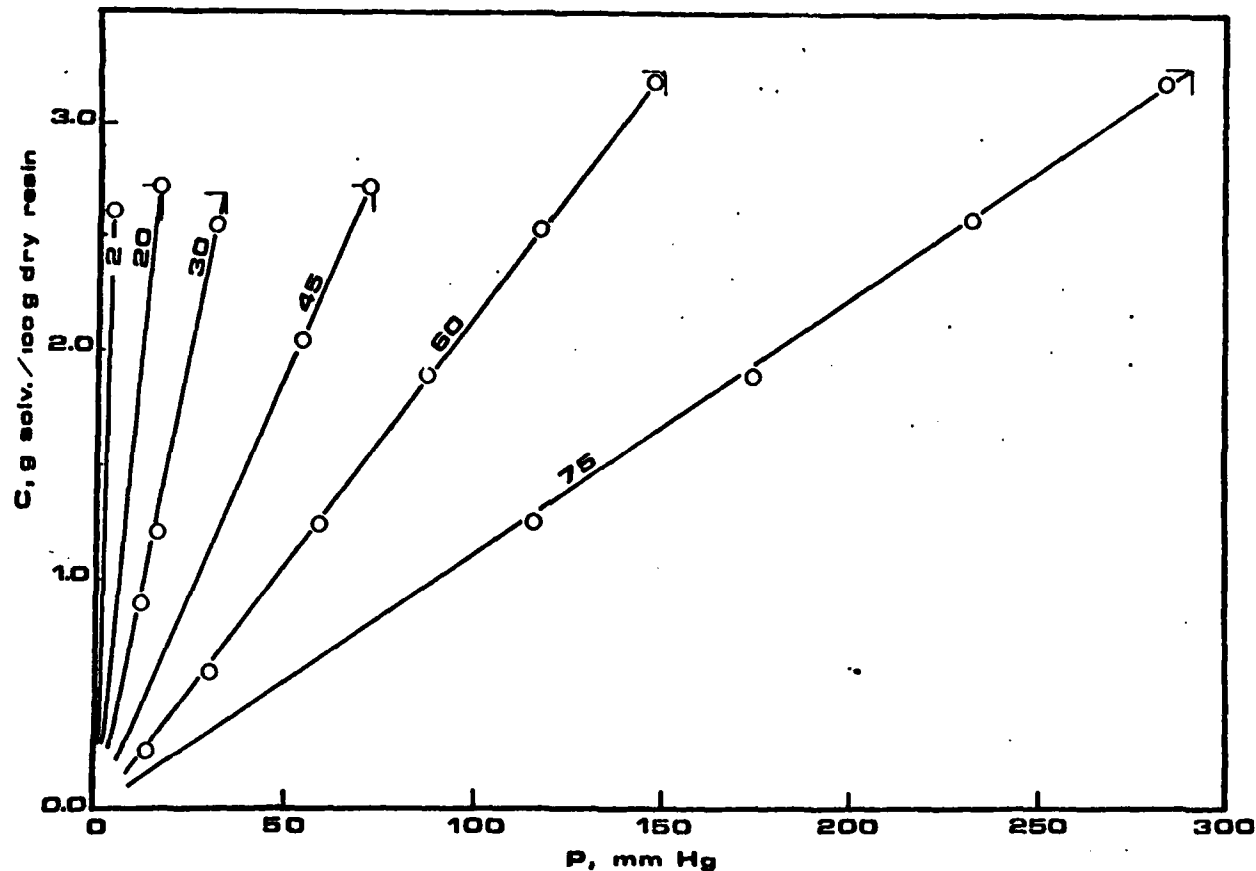


Figure 15: Equilibrium solubility isotherms as a function of the actual water vapour pressures.

Conversely, a straight line correlated well the solubility constants of the resins referred as "undamaged" (low temperature and activity tests) and reported in Figure 16. The increase in the apparent solubilities and the upward shape of the isotherms may be attributed to irreversible morphological changes occurring in the bulk polymer at increasingly higher humidities and temperatures.

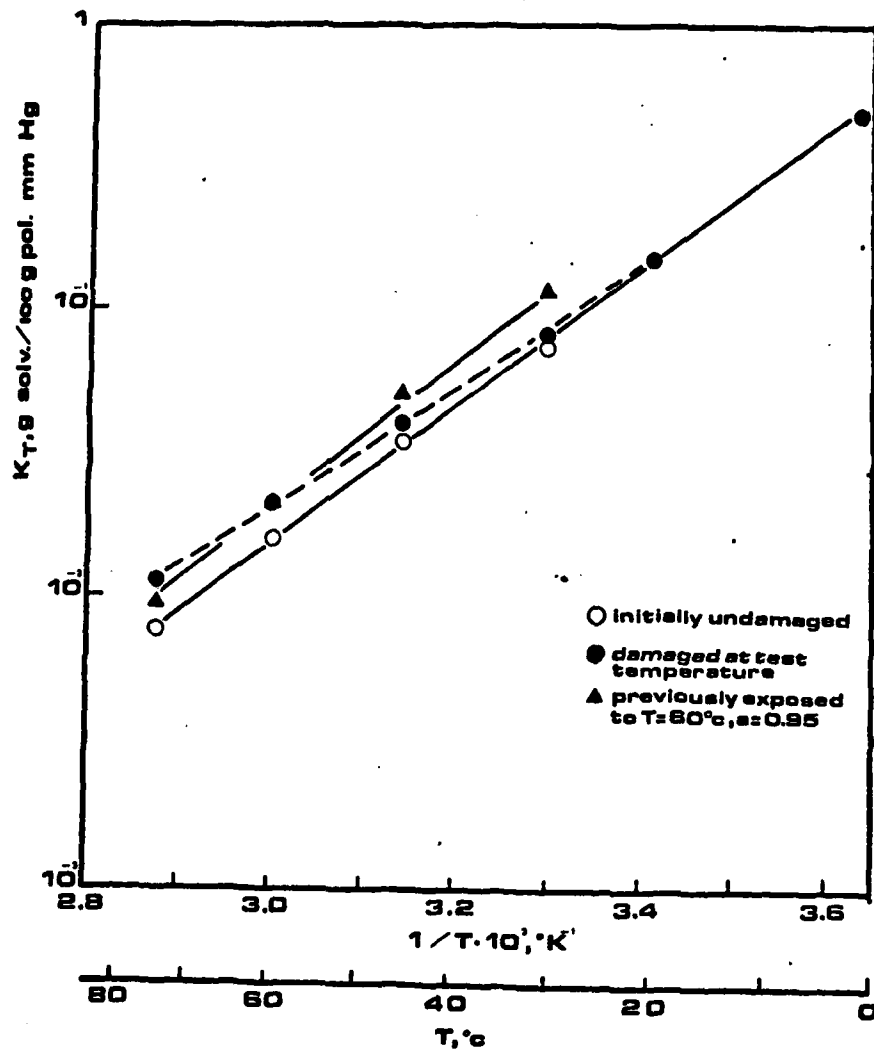


Figure 16: Apparent Henry's constants as a function of the reciprocal of the Temperature obtained from the initial linear portion of the upward isotherms (undamaged) (O), linear isotherms (damaged) (●) and linear isotherms for specimens previously exposed at  $60^\circ\text{C}$  and R.H. 99% (▲).

However, once the state of the material has been fixed by the hygro-thermal history, again a linear relationship should be found. The solubility isotherms for tests performed at  $30^{\circ}\text{C}$  and  $45^{\circ}\text{C}$  on samples previously equilibrated at  $60^{\circ}\text{C}$  and at an activity of 0.99 are reported in Fig. 17.

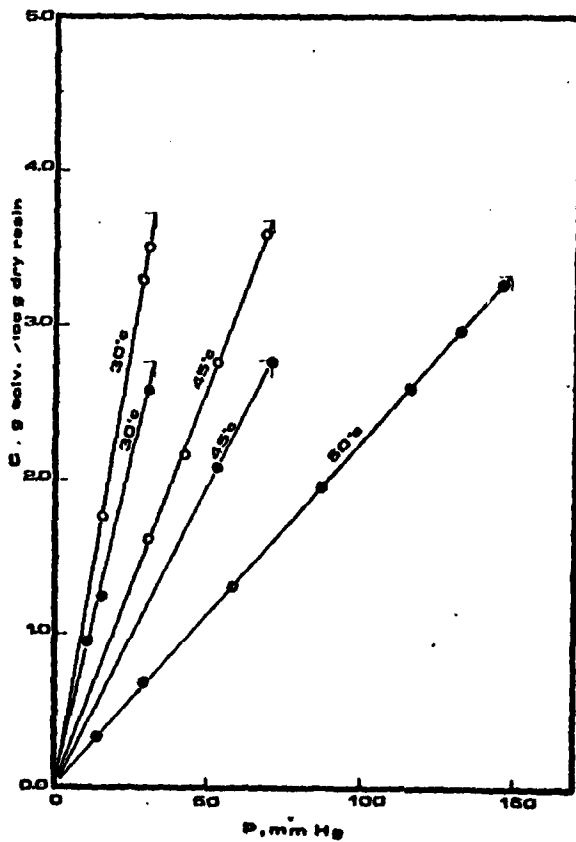


Figure 17: Comparison between the linear isotherms at  $45^{\circ}$  and  $30^{\circ}\text{C}$  for samples equilibrated at the test temperature (●) and previously equilibrated at  $60^{\circ}\text{C}$  and R.H. 99% (○).

For such system, linear isotherms have been observed and are compared, open circles in Fig. 17, with those obtained for samples equilibrated at the test temperature only,  $45^{\circ}$  and  $30^{\circ}\text{C}$ , (full circles). For the system previously equilibrated at  $60^{\circ}\text{C}$ , the higher degree of damage is shown by a higher solubility constant.

The overall apparent Henry's law constants, obtained from Fig. 17 and at 75°C from a low activity ( $a = 0.20$ ) experiment on a sample previously equilibrated at 60°C and  $a = 0.99$ , are reported as full triangles in Figure 16. As expected, a straight line, parallel to the one corresponding to the undamaged resin, well correlates the higher values of the apparent solubilities found for samples of a fixed damage.

#### Sorption kinetics

Equilibrium moisture sorption levels were found (36) to be represented, for the same polymer and at the same temperature and humidity conditions, both by linear and upward isotherm, i.e. Fig. 10, depending upon the humidity history to which the system was subjected.

In first sorption on "as cast" resins (open circles) the initial apparently linear isotherm (dotted line) was progressively subject to significant positive deviations, associated with a damaging process as the external activity was increased over 0.60. Once the maximum humidity level imposed to the system is fixed, for all subsequent sorption and desorption the solubility data were fitted by linear isotherm (full circles and triangles). In Fig. 10, vapor sorption data for high activities and temperatures in the first sorption run were not described by ordinary Fick's laws. An explanation of such anomalous behavior will be given further on, using the arguments discussed in the previous section. Moisture sorption and desorption kinetics for two different values of the activity in "as cast" epoxy resin (first sorption-desorption cycles) are reported in Fig. 18 for tests made at  $T = 75^\circ\text{C}$ .

According to ordinary Fickian diffusion with constant diffusion coefficient, both an initial linear part in a weight gain vs  $t^{\frac{1}{2}}$  plot and sorption and desorption data lying on the same curve are expected.

However, while this is verified at low activities ( $a = 0.60$  in Fig. 18), at higher activities ( $a = 0.80$ ) anomalous behavior has been found.

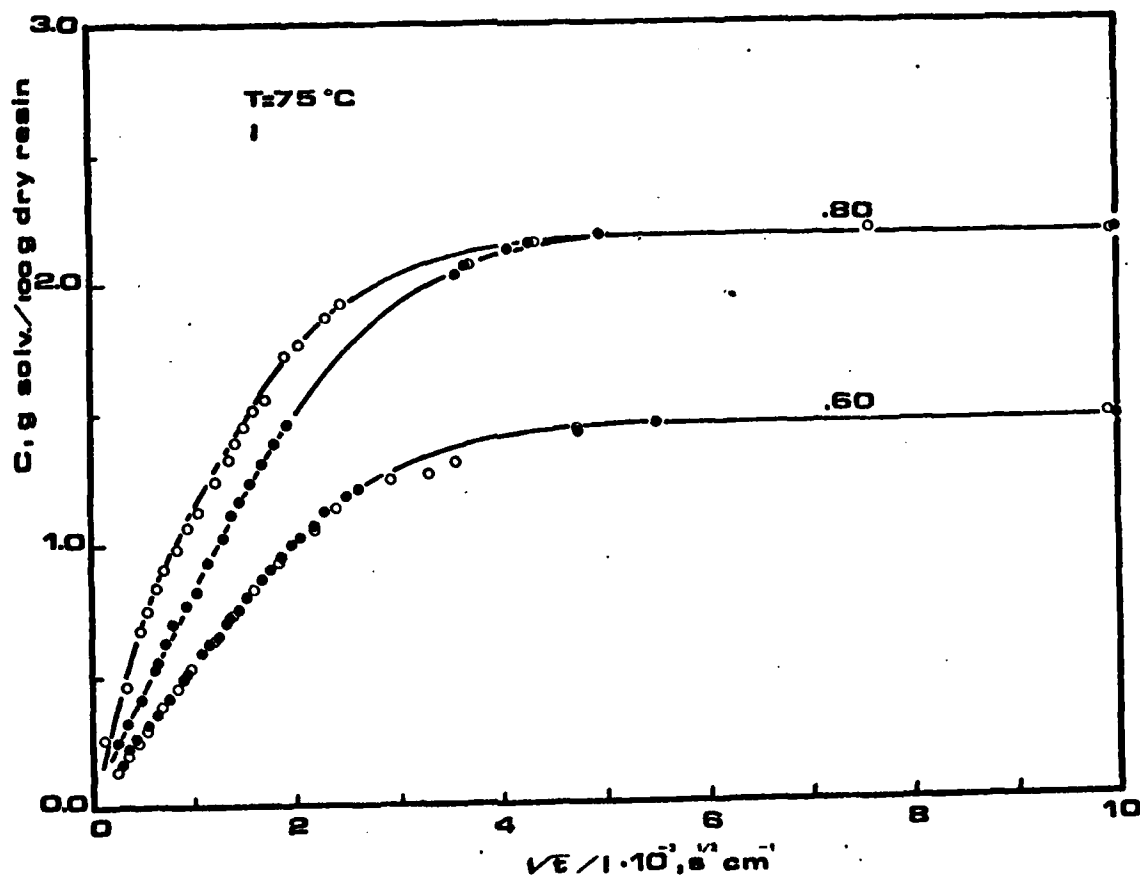


Figure 18: Moisture sorption (○) and desorption (●) kinetics for the "as cast" resin at two different external activities.  $T=75^\circ\text{C}$ .

As previously discussed the effect of damaging processes on the effective diffusion coefficient may be attributed to morphological changes in form microcavities. The anomalous behavior shown in high humidity environments could, in principle, be also explained by an effective concentration dependence of diffusion coefficients.

Sorption and desorption tests performed at the same high activity ( $a = 0.80$ ) and temperature on a sample previously equilibrated at  $a = 0.99$  (second circle runs) are shown in Figure 19.

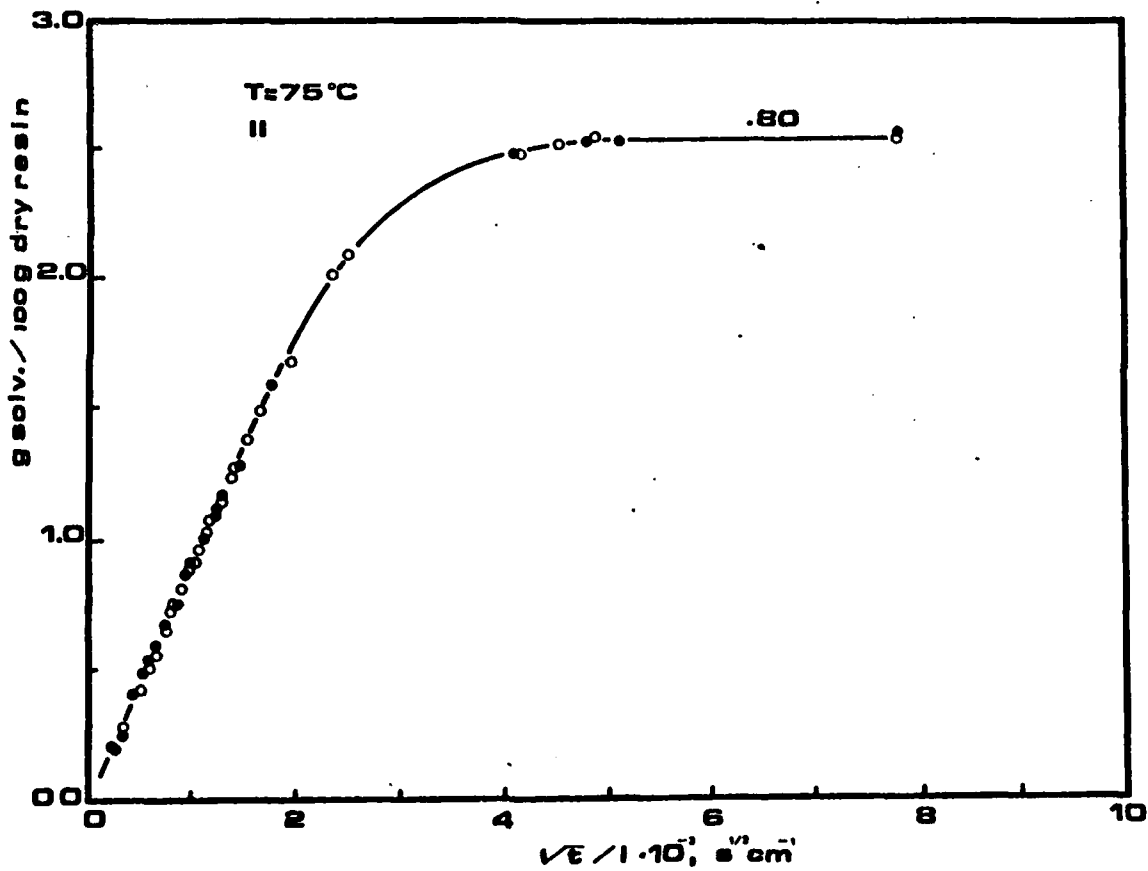


Figure 19: Moisture sorption (O) and desorption (●) kinetics for a previously equilibrated at  $75^\circ\text{C}$  and 99% R.H. sample. External activity 0.80.

A good superposition of the sorption and desorption data may be observed as predicted by the proposed model, since no additional microvoid formation is expected once the material has already been exposed to more severe conditions. In addition, this result indicates that the use of a real concen-

tration dependent diffusion coefficient would not be satisfactory to explain the anomalies found in Fig. 19. Moreover, the environmental conditions of  $a = 0.60$  and  $T = 75^\circ\text{C}$  are not able to induce significant microvoiding in the resin since evident anomalies have not been found in the sorption curves.

Sorption curves obtained at the same activity,  $a = 0.60$  and  $T = 75^\circ\text{C}$ , for "as cast" samples (A) and for a sample previously equilibrated at  $a = 0.99$  at the same temperature (B) are shown in Figure 20.

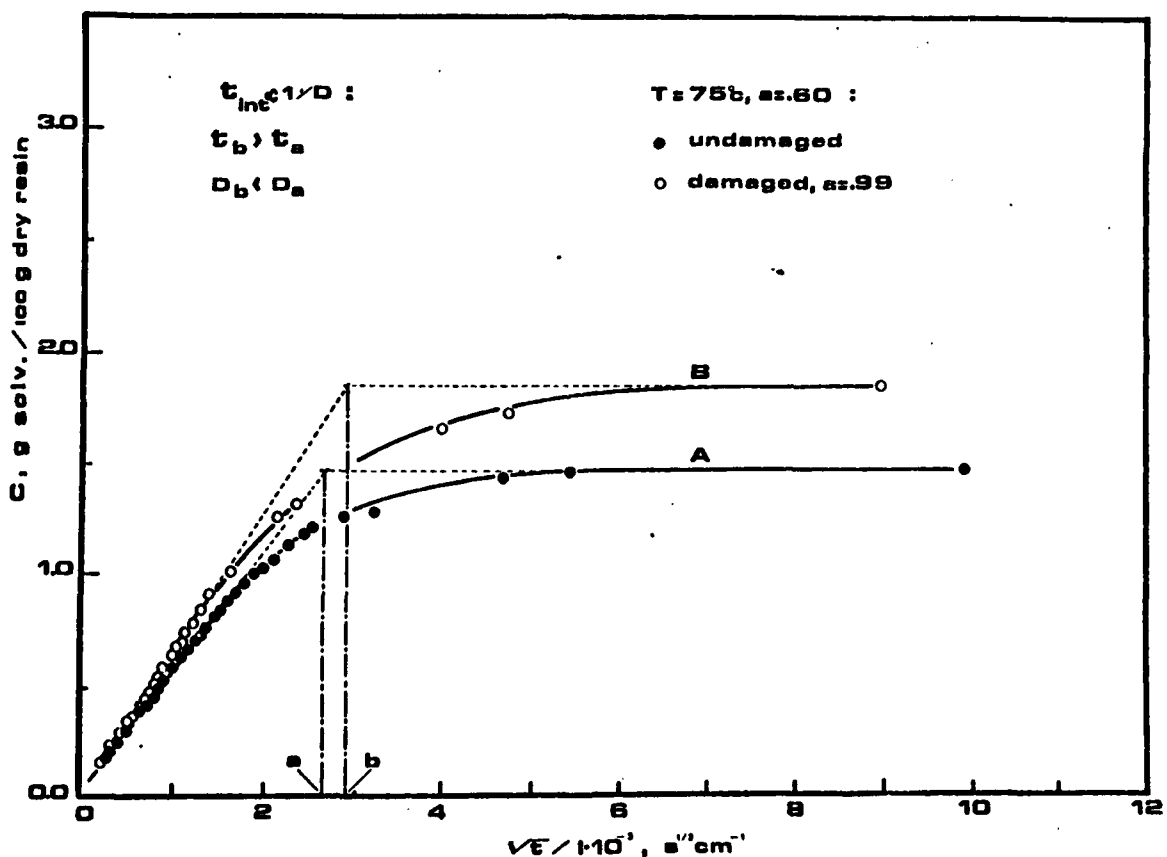


Figure 20: Comparison between moisture sorption kinetics in the same external condition for sample with different previous histories.

It can be observed, as according to Eq. 8, that the diffusion coefficient of the damaged sample is lower than that of the undamaged specimens ( $b > a$ ). The morphological modification which increases the solubility of the crazed resin, at fixed environmental conditions, lowers the effective diffusion coefficient.

In Figure 21 the ratios between diffusion coefficients obtained in the same experimental conditions, on samples equilibrated in different environmental conditions, are reported as a function of the ratios between the measured solubilities and are compared with Eq. 8 (full line). The agreement between the experimental data and the theory is fairly good.

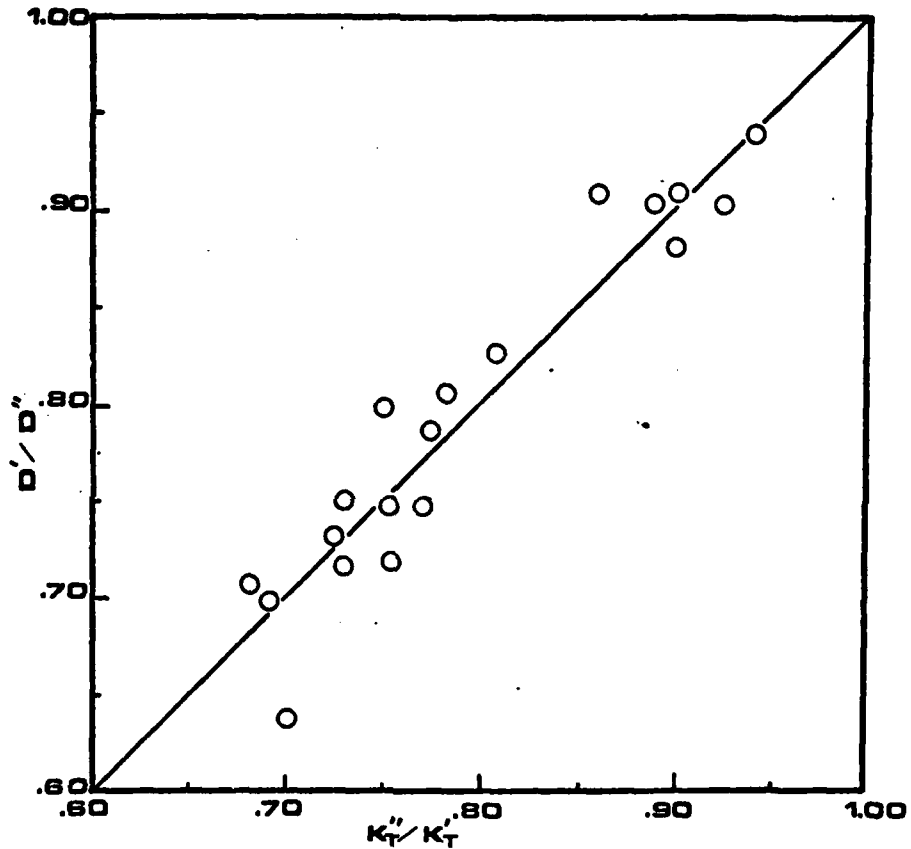


Figure 21: Diffusion coefficient depressions  $D'/D''$  vs solubility increases  $K''_T/K'_T$ : (O) experimental, (—) equation 8.

As previously reported the damaging process is not evident at low external humidity levels for all the temperature investigated, and at low temperatures for all relative humidities analyzed. As a consequence, effective diffusion coefficients for the undamaged polymer can be calculated at high temperatures in low humidity environments and at low temperatures in all humidity conditions (also liquid water).

Diffusion coefficients for damaged ( $T = 60^{\circ}\text{C}$ ,  $a = 0.99$ ) and undamaged

resin have been crossplotted with solubility data, as a function of the reciprocal of the temperature.

As for the solubility data, open triangles in Figure 22, the diffusion coefficients calculated from tests performed both at low temperatures (2 and 20°C) in liquid water and at high temperatures and low activities (referred as undamaged), are also well correlated by a straight line in the Arrhenius plot (open circles in Fig. 22).

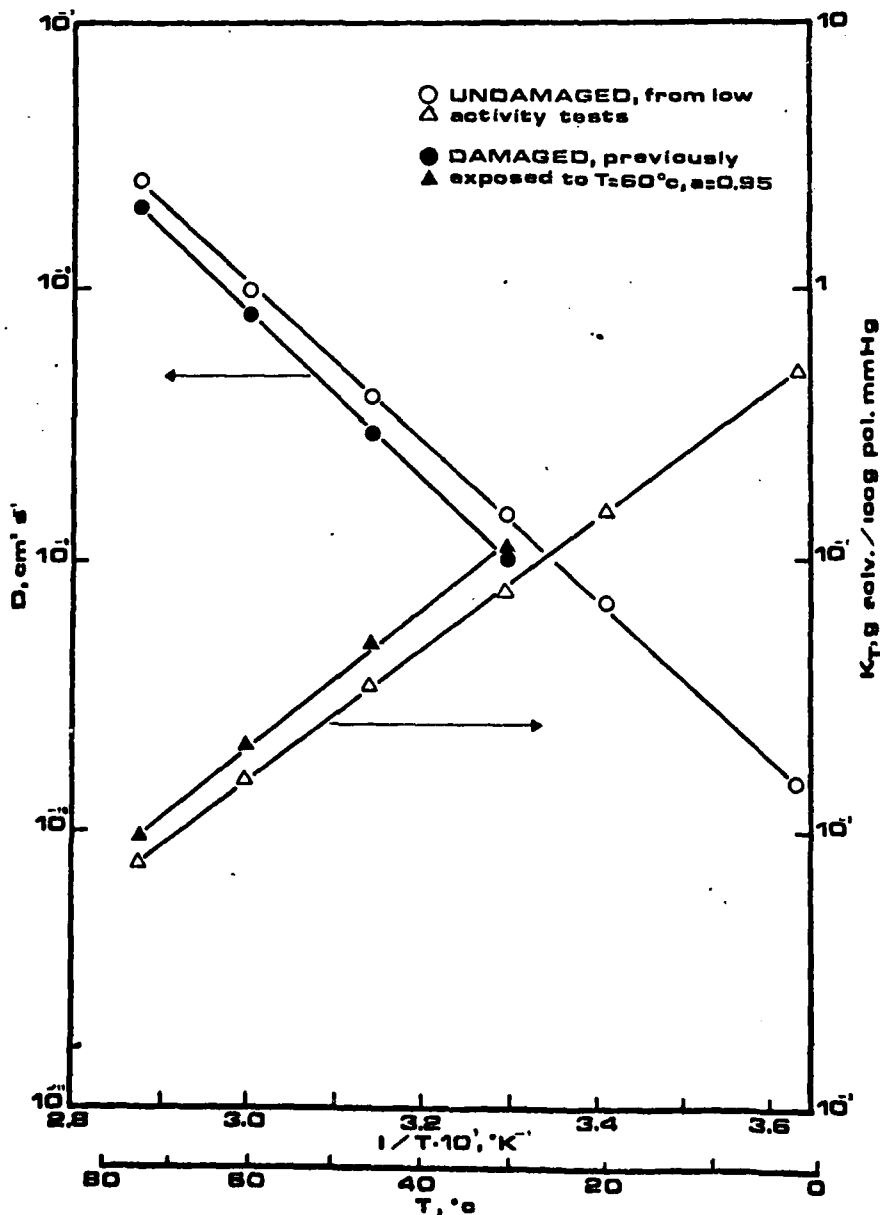


Figure 22: Crossplot of the Diffusion coefficients and solubilities as a function of  $1/T$  for undamaged ( $\textcircled{O}, \triangle$ ) and damaged at  $60^\circ\text{C}$  and 99% R.H. ( $\bullet, \blacktriangle$ ) epoxy samples.

For damaged samples lower diffusion coefficients (full circles) and higher solubilities (full triangles) have been found in the range of the temperatures studied. An activation energy for the diffusion process of about 13.5 Kcal/mole has been calculated both for damaged and undamaged samples. The corresponding enthalpy of sorption for both materials has been found to be -11.0 Kcal/mole.

In conclusion sorbed moisture induces different degree of irreversible damage on the resin depending upon the temperature and humidities imposed to the sample. At low temperatures ( $T < 20^{\circ}\text{C}$ ) or at low R.H. (< 50%), moisture sorption was not found to be effective in the damaging process. Moisture sorption isotherms were, indeed, found non linear (upward) showing positive deviations from linearity only at R.H. greater than 50%. However, once the maximum value of the R.H. was experienced by the sample, equilibrium weight gains were again found to be linear with the R.H.

The difference in the sorption behavior in the same environmental conditions (but before and after moisture conditioning) have been associated with a progressive damage produced in the material equilibrated at increasingly higher moisture contents. Furthermore, the differences between the linear and upward isotherms were less pronounced at low temperatures where, as discussed in the previous section, a lower damaging tendency has been noted.

Sorbed moisture as well as temperature "per se" are not effective in producing any microcavitation in the resins but the synergistic action is really active in the damaging process.

For the damaged samples lower diffusion coefficient and higher solubilities than in the undamaged state were observed. The nature of the hypothesized damaging process was then in agreement with the diffusion coefficient depression experimentally found and theoretically predicted by the analysis based on the Dual Mode Sorption transport model (28-29).

APPLIED STRESS AND DAMAGING PROCESS IN PRESENCE OF SORBED MOISTURE

Crazing has been described as a form of yielding in glassy polymers involving significant cavitation and localized fibrillation and orientation of the material surrounding the cavities (33) which develops a thermodynamic restoring force due to conformational entropy changes of the oriented macromolecules. However, in ordinary conditions crazing is considered irreversible since the weakness of the restoring force as related to the forces required to initiate the cavitation, results in a recovery time scale that is decades longer than the typical initiation time scale. In addition, while cavitation is isotropic in character, the fibrillation and orientation of craze surrounding the cavities is not, and, in fact, its directionality has been described (44) in terms of major principal stress always perpendicular to the craze tip, hence the name normal stress yielding (45). For these reasons a criterion for crazing based entirely on the first invariant is not adequate, implying that craze formation should be a completely isotropic yielding process.

The dependence of craze initiation has been successfully described in terms of deviatoric stress bias ( $\sigma_b$ ) versus the reciprocal of the first-stress invariant ( $I_1$ ) (45). The stress bias (i.e. stress vector with magnitude equal to the major shear stress but with direction of the major principal stress), may be viewed as the driving force, and as direction determining component of the stress state, for the fibrillation and orientation step, whereas the first-stress invariant is the cavitation driving force.

In equation form it may be expressed as:

$$\sigma_b > A + \frac{B}{I_1}$$

where A and B are temperature-dependent material constants and  $I_1$  is the first-stress invariant which must be positive (dilational) for cavitation. This suggests that as the stress field becomes non dilational, the cavitation process is the limiting factor, craze becomes increasingly difficult to initiate and shear yielding may be observed as yielding mode (45).

The above criteria may be qualitatively used to investigate the nature of the damaging process associated with moisture sorption. In fact, if craze formation is invoked to explain apparent solubility changes of samples subjected to different hygrothermal histories, the effects of an externally applied stress field on solubilities may be predicted, considering its influence on the driving force for cavitation,  $I_1$ .

Sorbed solvent induced osmotic stresses or differential swelling strains of regions with different crosslinking densities (4,23) produce the "internal" stress field distribution responsible for craze formation. The superposition of an external stress field will favor or decrease the tendency of the material to craze, depending on the variations of the resulting first-stress variant. For example, the application of a tensile stress will increase  $I_1$  and a more crazed (damaged) material should be obtained, while, conversely, the application of a hydrostatic pressure will decrease  $I_1$  and a less crazed material should result. Such an expectation has been experimentally tested by performing sorption experiments on samples subjected to different "stress histories" when exposed to the same environmental conditions. Liquid water sorptions have been previously carried out at  $T = 40^\circ\text{C}$  on an uniaxially loaded dumbbell sample and on an unloaded reference sample. After a period three times longer than usually needed to equilibrate unloaded samples at the same temperature, the dumbbell specimens were cut into rectangular shapes and weighed in the wet state. The dry weight was subsequently obtained after a drying procedure under vacuum at  $T = 40^\circ\text{C}$  until no weight changes were further observed. Weight gains subsequent to resorption from liquid water at  $T = 40^\circ\text{C}$  were then followed for the two samples with different stress histories, and are reported in Fig. 23. The previously loaded and water penetrated sample clearly shows a higher solubility than the unloaded sample.

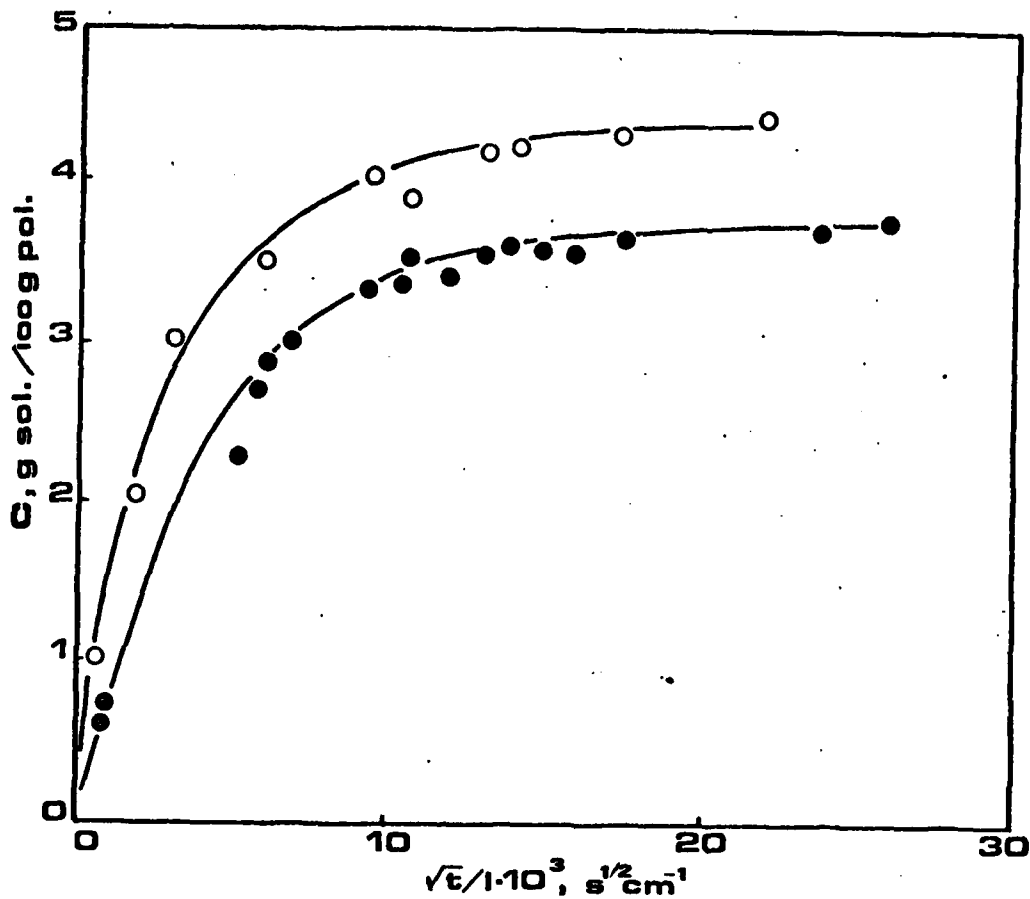


Figure 23: Liquid water uptake in resorption tests performed on previously saturated in water and dessicated samples at 40°C. Previously loaded ( $\sigma = 0.30 \text{ Kg/mm}^2$ ) (○) and unloaded (●) samples.

In Table 3 the applied stress, equilibrium moisture uptakes and percent solubilities increases are reported for the loaded and unloaded samples.

Applied stress, $\text{Kg/mm}^2$	Apparent solubility, g water/100g dry polym.	C, %
0	3.89	0
0.30	4.54	16.3

Table 3: Apparent solubility variations between loaded and unloaded samples exposed to liquid water at 40°C.

An increase of about 16 percent of the apparent solubilities has been found after applying a stress that is only 7 percent of the yielding stress for a saturated sample (46) or 5 percent of the  $\sigma$  break for a dry

sample (46). Local yielding in form of crazes may be possible since, for the applied stress used, we are well inside the linear elastic region of the stress-strain curve (46).

The increase in "crazeability" expected as a consequence of the increase of the driving force for cavitation,  $I_1$ , is experimentally evident in an apparently higher solubility of the loaded samples.

In conclusion, sorption experiments, performed on samples subjected to different "stress histories" during the exposure to the same environment, shown as the previously loaded and water penetrated samples clearly sorb more water than the unloaded samples. The application of a tensile stress in the glassy systems resulted in an effective dilatation of the sample (Poisson ratio 0.3), and the increase of the driving force for cavitation.

#### DAMAGING OF EPOXY COMPOSITES

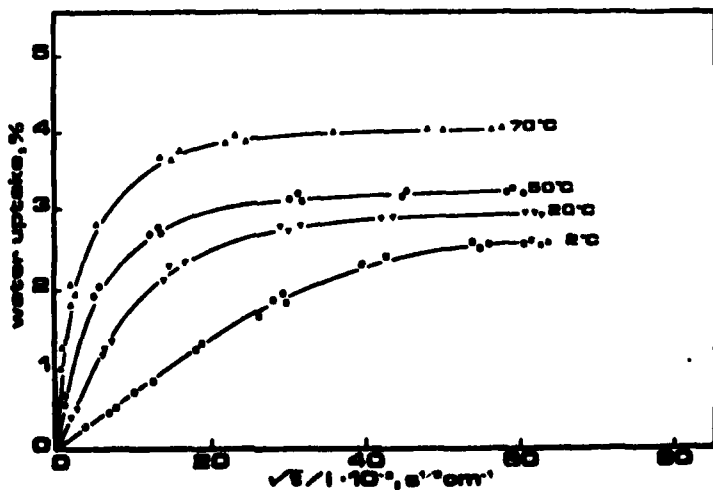
The presence of rigid fillers may enhance the microvoid formation in regions where stresses are concentrated. Recognition that crazing requires void formation leads, in fact, to the suggestion that the phenomenon should be favored (44) in the presence of a dilatational component of the stress.

As shown before, the previously loaded and water penetrated epoxies clearly sorb more water than the unloaded ones in sorption experiments performed on unfilled epoxy samples subjected to different "stress histories".

The purpose of the final part of the work is to separate the effect of the plasticization in epoxy composites and the crazing by analyzing the recoverable mechanical property losses due to plasticization, which is a reversible phenomenon, and those due to the microcavitation which is not recoverable.

Moreover, the internal tensile stresses, like those arising from the shrinkage of the glassy matrix around fillers, further increases the polymer tendency to craze, decreasing the recoverable strength of the composite.

Liquid water sorptions were carried out on glass bead epoxy composites and unfilled epoxy films from the same batch of resin at temperatures ranging from 2 to 70°C. The sorption kinetics for the unfilled epoxies at 2, 20, 50 and 70°C are reported as a function of the square root of time normalized to the sample thickness in Fig. 24.



Sorption curves in Fig. 24 appear Fikian and progressively higher water uptakes were achieved by the samples saturated at progressively higher temperatures.

As extensively described in the previous sections, moisture sorption is often accompanied by a microvoiding damage of the resin which, especially at high temperatures, increases the equilibrium water uptakes. The amount of water actually dissolved in the resin should be calculated in the hypothesis that the excess of water was trapped in the crazed regions. Figure 25 shows the stress-strain behavior of the dry and water conditioned epoxy matrix.

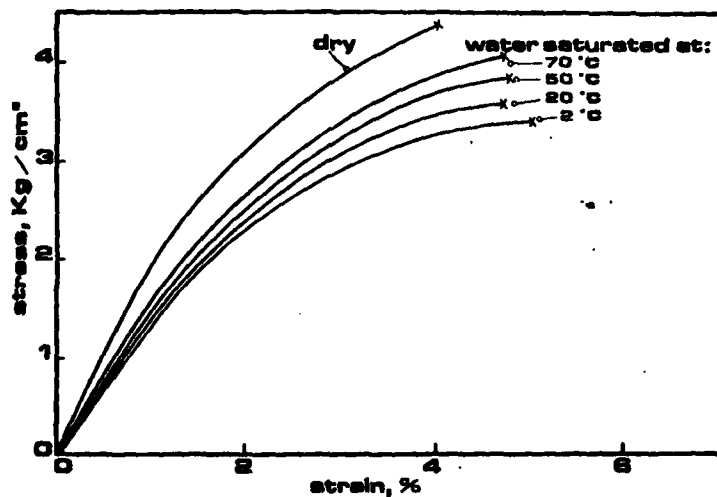


Figure 25: Stress-Strain behaviour at 20°C of the dry and saturated in liquid water epoxies.

Table 4 reports the apparent water solubilities  $S_{app}$ , and some characteristic mechanical properties at 20 and 50°C of the samples equilibrated at the four temperatures. On the same Table the mechanical properties of the "as cast" dry resins are compared with those obtained for the wet samples. The mechanical tests were performed for the wet resins in 100% Relative Humidity environments thermostated at 20 and 50°C. The time of the test was found to be too short to induce appreciable variations of both the effective and actual water contents. The stress-strain curves for the dry and water conditioned specimens are reported in Fig. 25. The elastic modulus and the stress at break (see Table 4), progressively, increase for the samples equilibrated at increasing temperatures, in contrast to the higher

water uptakes. For example, the sample equilibrated at 2°C, which has the lower apparent water content, shows the higher degree of plasticization at both temperatures, while, conversely, the opposite behavior is found for the resin normalized at 70°C.

WATER CONDITIONING	$S_{app'}$	E, Kg/mm <sup>2</sup>	$\sigma_b'$ , Kg/mm <sup>2</sup>		$\epsilon_b'$ , %	
			@20°C	@50°C	@20°C	@50°C
TEMPERATURE °C	%					
2	2.58	139	76	3.40	2.40	4.9
20	2.96	149	92	3.58	2.70	4.5
50	3.22	156	105	3.80	2.92	4.4
70	4.00	179	112	4.05	3.10	4.5
DRY	-	216	129	4.40	3.40	4.0

Table 4: Mechanical properties at 20°C and 50°C and apparent solubilities of unfilled epoxy resins equilibrated in liquid water at increasing temperatures.

The elongation at break,  $\epsilon_b$ , is less sensitive to the degree of plasticization than the elastic modulus and  $\sigma_b$ .

The presence of a volume percent of microvoids lower than 1.5 should not significantly decrease the mechanical properties.

From the data of Table 4 it appears that the higher degree of plasticization is reached after the exposure to liquid water at the lower temperatures. The water actually dissolved in the resin seems to be a decreasing function of the temperature while the excess of water, which is associated with the not recoverable damage, conversely, increases at higher temperatures. Similar conclusions have been previously proposed (10) from the analysis of the sorption behavior of the unfilled resin during the thermal cycling of the wet samples from higher to lower temperatures. The same experiments which were performed from 70° to 20°C on the resin and a glass bead composite (7.5 volume percent), are reported in Figure 26. The

samples equilibrated at 70°C, when brought down to 20°C (right part of Figure 26), both sorbed 0.60% of additional water. The equilibrium values reached by the composite first equilibrated at 70°C and then at 20°C are indicated as "b" and "a" in Fig. 26. The values relative to the unfilled resin are reported as "d" and "c" in the same Figure, while "e" indicates the equilibrium solubility reached at 20°C by the "as cast" resin. The water uptakes for the composite are referred to the dry weight of polymer. The two kinetic curves at 70°C strongly differ in the final sorption stages while behave similarly in the initial part.

At equilibrium, the two curves show a difference of about 1% ( $b > d$ ) in the water uptakes (4% for the resin and 5% for the composite). Such difference was maintained when the same samples were subsequently conditioned at 20°C ( $a > c$ ), (4.60 for the resin and 5.60 for the composite).

Water sorption is a slightly exothermic process for this epoxy resin (36) and higher solubilities have been, in fact, found at lower temperatures to explain the increases in the water uptakes.

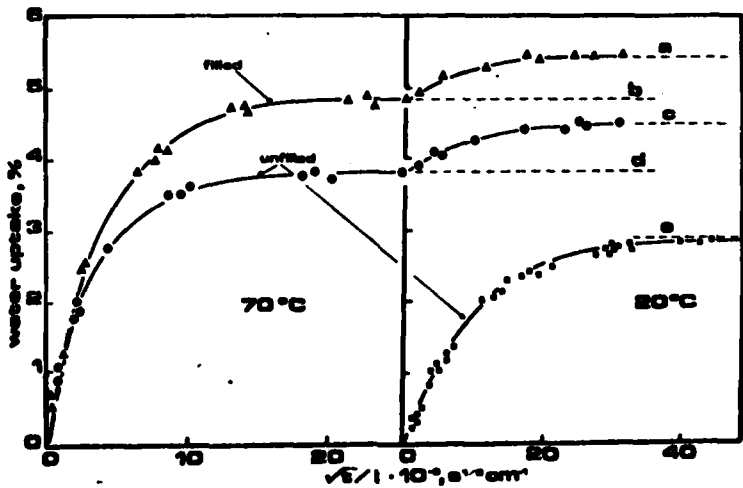


Figure 26: Comparison between the liquid water sorption behavior of the unfilled (●) and glass bead composite (▲) at 70°C (left). Sorption behavior at 20°C of the "as cast" (■), saturated at 70°C resin (●) and composite (▲) at 20°C.

The polymeric component of the composite exposed in water at  $70^{\circ}\text{C}$  sorbs about 90% more than the unfilled "as cast" resin conditioned directly at  $20^{\circ}\text{C}$ . The large excess of water found for the composite could be attributed to a significantly increased microvoiding damage due to the presence of the filler. The unfilled but previously exposed at  $70^{\circ}\text{C}$ , in fact, sorbs at  $20^{\circ}\text{C}$  only, 60% more water than the unfilled resin conditioned directly at the same temperature.

The residual stresses induced around the inclusion by the shrinkage of the resin during the curing favor localized crazing (36) if the composite is exposed to a severe environment. Mechanical tests and Scanning Electron Micrographs have been used to evaluate the localization of the damage. Figure 27 shows the stress-strain curves at room temperature of the pure resin and the composite in the "as cast" and water conditioned at  $70^{\circ}\text{C}$  states. The presence of the inclusions increases the elastic modulus of the dry sample (curves a and b), but strongly decrease it and embrittle the composite after the aging (curves c and d). The role of the water plasticization and crazing on the mechanical properties of the

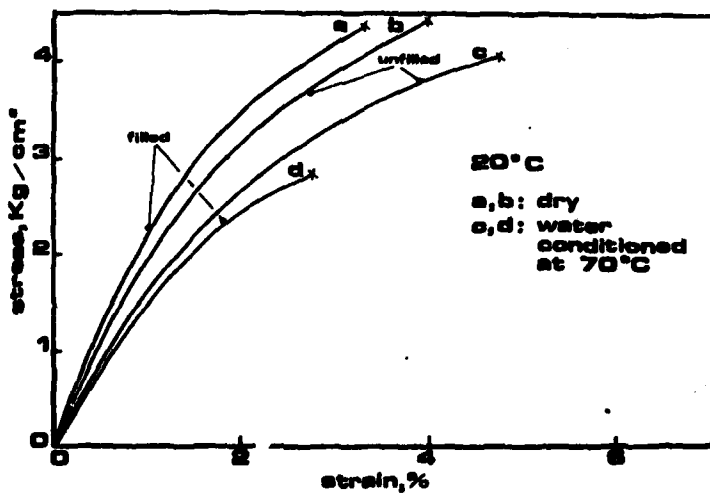


Figure 27: Stress-Strain behavior at  $20^{\circ}\text{C}$  for the unfilled resin (b and c) and composite (a and d) before (a and b) and after (c and d) the liquid water conditioning at  $70^{\circ}\text{C}$ .

matrix and the composite aged at 50°C and 70°C is summarized in Table 5. For example, the decrease of 17% of the elastic modulus of the wet unfilled resin conditioned at 70°C should be attributed to the plasticization only, while the reduction of 34% observed for the wet composite contains both the contributions due to the plasticization and to the localized crazing.

	Test Temperature 50°C				Test Temperature 20°C			
	Dry		Saturated @ 50°C	Saturated @ 70°C	Dry		Saturated @ 50°C	Saturated @ 70°C
	volume %	0 7.5	0 7.5	0 7.5	0 7.5	0 7.5	0 7.5	0 7.5
E, Kg/mm <sup>2</sup>	129 175	105 115	112 127		216 250	156 143	179 164	
$\sigma_b$ , kg/mm <sup>2</sup>	3.40 3.17	2.29 2.20	3.10 2.27		4.40 4.30	3.80 2.80	4.05 2.85	
$\epsilon_b$ , %	4.2 3.0	5.4 2.6	5.3 2.4		4.0 3.3	4.4 2.9	4.5 2.7	

Table 5: Mechanical properties at 20° and 50°C of the unfilled resin and the glass bead composite equilibrated in liquid water at 50° and 70°C. The data of the "as cast" dry sample are also reported.

The Scanning Electron Micrographs of the fracture surfaces of the undamaged, Figure 28a, and water conditioned at 70°C, Figure 28b, composites indicate that the damage is confined around the inclusions.

The adhesion between the matrix and the fillers seems to be weaker than the bulk strength for the unconditioned samples, while it seems to become relatively stronger when the matrix is locally deteriorated (crazed). The unconditioned fractured composite shows "clean" bead surfaces, Figure 28a, while the conditioned composite has fragments of the bulk resin adherent to the fillers, Figure 28b.



**Figure 28: Fracture surfaces of glass bead composites at 20°C:  
a, "as cast" and b, conditioned in liquid water at 70°C.**

The increased loss of the elastic modulus observed for the high temperature aged samples should be attributed to the lower number of beads acting as effective reinforcements.

In conclusion, the presence of rigid fillers in a epoxy matrix, under the action of an aggressive environment, fastens the aging of the composite. The damage is concentrated around the inclusions where the penetrant is concentrated. Such a behavior could be attributed to the synergistic action of water diffusion, temperatures and stresses.

REFERENCES

- 1) E.L. Mc Kague Jr, J.E. Halkias and J.D. Reynolds, J. Composite. Mat., 9, 2 (1975)
- 2) Chi - Hung and G.S. Springer, J. Composite Mat., 10, 2 (1976)
- 3) Y. Weitman, J. Composite Mat., 10, 193 (1976)
- 4) R.J. Morgan and J. O'Neal, J. Mat. Sci., 12, 1966 (1977)
- 5) O. Ishai and U. Arnon, ASTM STP 658, J.R. Vinson Ed. Am. Soc. for Tests. Mat., 1978, pagg. 267-276
- 6) C.E. Browning, Polymer Eng. Sci. 18, 16 (1978)
- 7) A.C. Loos and G.S. Springer, J. Composite. Mat., 13, 17 (1979)
- 8) J.D. Keenan, J.C. Seferis and J.F. Quinlivan, J. Appl. Polym. Sci., in press.
- 9) O. Ishai and U. Arnon, J of Testing and Evaluation, 5, N. 4, 320 (1977)
- 10) A. Apicella, L. Nicolais, G. Astarita and E. Drioli, Polymer, 20, 9 (1979)
- 11) A.S. Michaels, H.J. Bixler, H.B. Hopfenberg, J. App. Pol. Sci., 12, 991 (1968)
- 12) G.A. Pogany, Polymer, 17, 690 (1976)
- 13) P.G. Le Grand, R.P Kambour, W.R. Haaf, J. Pol. Sci. A2, 1565 (1972)
- 14) A.C. Newns, Polymer, 16, 2 (1975)
- 15) T.K. Kwei, H.M. Zupko, J. Pol. Sci. A2, 7. 876 (1969)
- 16) A.R. Berens, H.B. Hopfenberg, Polymer, 19, 489 (1978)
- 17) H.B. Hopfenberg, R.H. Holley, V.T. Stannet, Pol. Eng. Sci. 9, 242 (1969)
- 18) L. Nicolais, E. Drioli, H.B. Hopfenberg, D. Tidone, Polymer, 18, 1137 (1977)
- 19) N. Thomas, A.H. Windle, Polymer, 19, 255 (1978)
- 20) L. Nicolais, E. Drioli, H.B. Hopfenberg, G. Caricati, J. Memb. Sci., 3, 231 (1978)

- 21) L. Nicolais, E. Drioli, H.B. Hopfenberg and A. Apicella, *Polymer*, 20, 459 (1979)
- 22) R.R. Kambour, E.E. Ramagosa, C.L. Grumer, *Macromolecules*, 5, 335 (1972)
- 23) U.T. Kreibich, R. Schimid, *J. Pol. Sci. Symposium* 53, 177 (1975)
- 24) A.S. Kenyon, L.F. Nielsen, *J. Macromol. Sci. Chem.* A3 (2), 275 (1969)
- 25) G.A. Gordon, *Polymer*, 18, 958 (1977)
- 26) A.C. Loos, G.S. Springer, *J. Comp. Mat.*, 13, 17 (1979)
- 27) E.L. Mc Kague Jr., J.D. Reynolds, J.E. Halkias, *J. App. Pol. Sci.*, 22, 1643 (1978)
- 28) V.T. Stannet, W.S. Koros, D.R. Paul, H.K. Lonsdale and R.W. Baker, in *Advances in Polymer Science*, H.J. Cantow, G. Dall'Asta, K. Dusek, J.D. Ferry, H. Fusita, M. Gordon, W. Kern, S. Okamura, C.G. Overberger, T. Saegusa, G.V. Shultz, W.P. Slichter, J.K. Stille (eds); Springer-Verlag Berlin 1979
- 29) W.R. Vieth, J.M. Howell, J.H. Hoseih, *J. Memb. Sci.* 1, 177 (1976)
- 30) A. Apicella, L. Nicolais, G. Astarita, E. Drioli, *Polym. Eng. Sci.*, 21, 18 (1981)
- 31) C.H. Shen and G.S. Springer, *J. Composite Mat.*, 10, 36 (1976)
- 32) E.L. Mc Kague Jr., J.D. Reynolds, and J.E. Halkias, *J. Eng. Mat. Techn.*, 48, H, 92 (1976)
- 33) R.P. Kambour, *Macromol. Revs.* 7, 1 (1973)
- 34) E.H. Andrews, G.M. Levy, J. Willis, *J. Mat. Sci.* 8, 1000 (1975)
- 35) "Environmental Aging of Epoxy Resins: Synergistic Effect of Sorbed Moisture, Temperature and Applied Stress", A. Apicella and L. Nicolais, A.C.S., I &EC Product Research and Development
- 36) K.J. Illers, *Macromol. Chem.* 127, 1 (1969)
- 37) W.R. Wieth, K.J. Sladek, *J. Coll., Sci.* 20, 1014 (1965)
- 38) D.R. Paul, W.J. Koros, *J. Pol. Sci. Phys.. Ed.*, 14, 675 (1976)

- 39) J.H. Petropoulos, J. Poly. Sci., A2 (8), 1797 (1970)
- 40) A.S. Michaels, W.R. Vieth, J.A. Barrie, J. Appl. Phys., 34, 13 (1963)
- 41) L.E. Nielsen, "Mechanical Properties of Polymers and Composites",  
Marcel Dekker, NY, 1974, Vol. 2, pag. 387
- 42) J. Crank, The Mathematics of Diffusion, Oxford Univ. press 1975
- 43) S.S. Sternstein, L. Ogechin, A. Silverman, Appl. Polym. Symp. 7, 175 (1975)
- 44) S.S. Sternstein , L. Ogechin, Poly.Prep. 10, 1117 (1969)
- 45) A.F. Lewis, M.J. Doyle, J.K. Gillham, Poly.Eng. and Sci. 19, 683 (1979)
- 46) L. Nicolais, E. Drioli, A. Apicella and O. Albanese, AFOSRTR-78-1429 (1978)
- 47) R. Hinrrichs, J. Thuen, paper presented at "VIII Inten. Congress of  
Rheology" Sept. 01-06-1980 Naples, Italy.

ATE  
LME